Measures of Cosmic Structure

Lecture course CSF2016
University Groningen
Nov. 2016-Jan 2017

Standard Reference:

Martinez & Saar

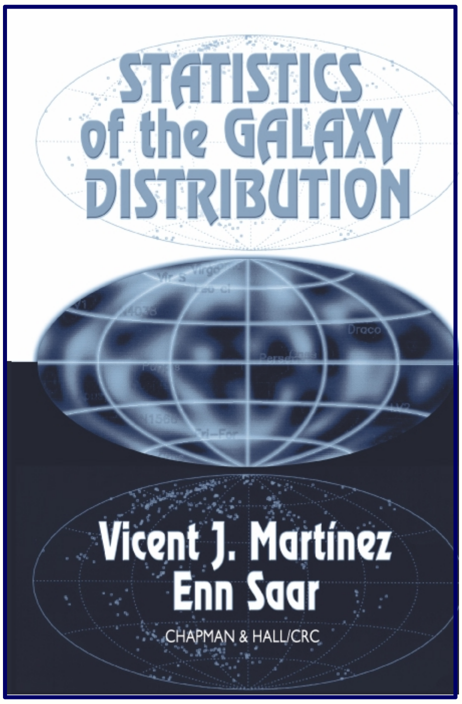

Ergodic Theorem

Statistical Cosmological Principle

Cosmological Principle:

Universe is Isotropic and Homogeneous

Homogeneous & Isotropic Random Field $\psi(\vec{x})$:

Homogenous $$p[\psi(\vec{x}+\vec{a})] = p[\psi(\vec{x})]$$

Isotropic $$p[\psi(\vec{x}-\vec{y})] = p[\psi(|\vec{x}-\vec{y}|)]$$

Within Universe one particular realization $\psi(\vec{x})$:

Observations: only spatial distribution in that one particular $\psi(\vec{x})$

Theory: $p[\psi(\vec{x})]$

Ergodic Theorem

Ensemble Averages ⟺ **Spatial Averages over one realization of random field**

- Basis for statistical analysis cosmological large scale structure
- In statistical mechanics Ergodic Hypothesis usually refers to time evolution of system, in cosmological applications to spatial distribution at one fixed time

Ergodic Theorem

Validity Ergodic Theorem:

- Proven for Gaussian random fields with continuous power spectrum
- Requirement:

spatial correlations decay sufficiently rapidly with separation

such that

many statistically independent volumes in one realization

⇩

All information present in complete distribution function $p[\psi(\vec{x})]$ available from single sample $\psi(\vec{x})$ over all space

Fair Sample Hypothesis

- Statistical Cosmological Principle

+

- Weak cosmological principle
  (small fluctuations initially and today over Hubble scale)

+

- Ergodic Hypothesis

fair sample hypothesis
(Peebles 1980)

Discrete e.g. Continuous

Discrete & Continuous Distributions

- How to relate discrete and continuous distributions:
- Define number density $n(\vec{x})$ for a point process:

$$n(\vec{x}) = \bar{n}[1+\delta(\vec{x})] = \sum_i \delta_D(\vec{x}-\vec{x}_i)$$

$\delta_D(\vec{x})$ Dirac Delta function

$\left\langle \sum_i \delta_D(\vec{x}-\vec{x}_i) \right\rangle = \bar{n}$ ensemble average

Correlation Functions

Correlation Functions

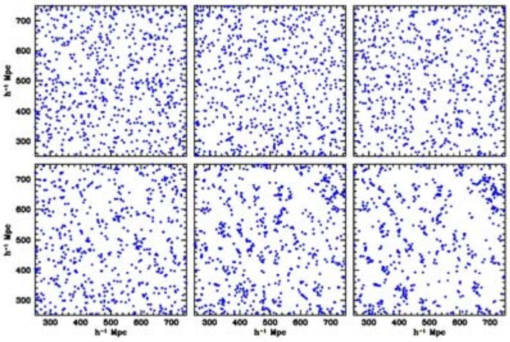

Joint probability that in each one of

the two infinitesimal volumes dV_1 & dV_2,

at distance r,

lies a galaxy

Infinitesimal Definition Two-Point Correlation Function:

$$dP(r) = \bar{n}^2 \left(1 + \xi(r)\right) dV_1 dV_2$$

mean density

Correlation Functions

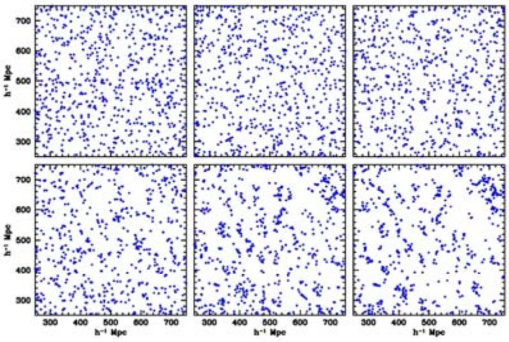

In case of Homogeneous & Isotropic point process

then $\xi(\vec{r})$

only dependent on

$|\vec{r}| = r$

Infinitesimal Definition Two-Point Correlation Function:

$$dP(r) = \bar{n}^2 \left(1 + \xi(r)\right) dV_1 dV_2$$

mean density

Correlation Functions

Discrete ⟺ Continuous

Two-point correlation function

$$dP(\overrightarrow{x_1}, \overrightarrow{x_2}) = \overline{n}^2 dV_1 dV_2 [1 + \xi(r_{12})]$$

$$r_{12} = |\overrightarrow{x_1} - \overrightarrow{x_2}|$$

$$\langle \delta(\vec{x}) \rangle = 0$$

Autocorrelation function

$$\xi(r_{12}) = \langle \delta(\overrightarrow{x_1}) \delta(\overrightarrow{x_2}) \rangle$$

probability for 2 points in dV_1 and dV_2

Correlation Functions

- Gaussian (primordial and large-scale) density field:

  Autocorrelation function ξ(r) Fourier transform power spectrum P(k)

$$\xi(\mathbf{r}) = \xi(|\mathbf{r}|) = \int \frac{\mathrm{d}\mathbf{k}}{(2\pi)^3} P_f(k) \mathrm{e}^{-\mathrm{i}\mathbf{k}\cdot\mathbf{r}}$$

  Autocorrelation function completely specifies statistical properties of field

- First order measure of deviations from uniformity

- Nonlinear objects (halos):
  ξ(r) measure of density profile

- Large Scales:
  related to dynamics of structure formation via e.g. cosmic virial theorem

Correlation Functions:
related measures

Other measures related to $\xi(r)$:

- Second-order intensity $\lambda_2(r) = \overline{n}^2 \xi(r) + 1$
- Pair correlation function $g(r) = 1 + \xi(r)$
- Conditional density $\Gamma(r) = \overline{n}(1 + \xi(r))$

Correlation Functions:
related measures

$$J_3(r) \equiv \int_0^\infty \xi(y) y^2 dy$$

Volume averaged correlation function $\overline{\xi}(r)$

$$\overline{\xi}(r) = \frac{3}{4\pi r^3} \int_0^r 4\pi \xi(x) x^2 dx = \frac{3 J_3(r)}{r^3}$$

Power-law Correlations

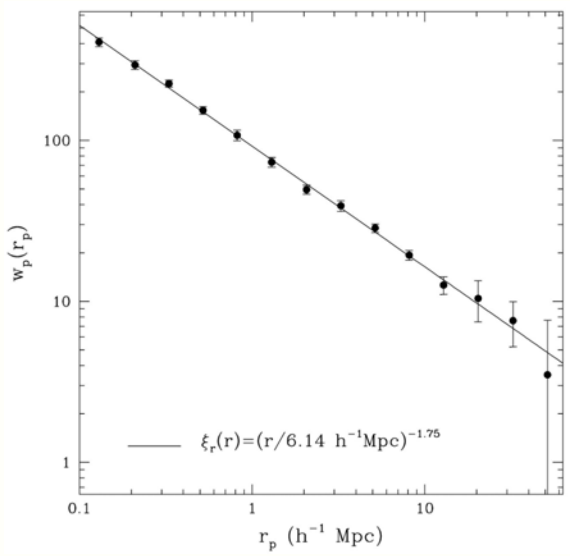

$$\xi(r) = \left(\frac{r}{r_0}\right)^{-\gamma}$$

$$\gamma \approx 1.8$$
$$r_0 \approx 5h^{-1}Mpc$$

Totsuji & Kihara 1969

Peebles 1975, 1980, …

Correlation Functions

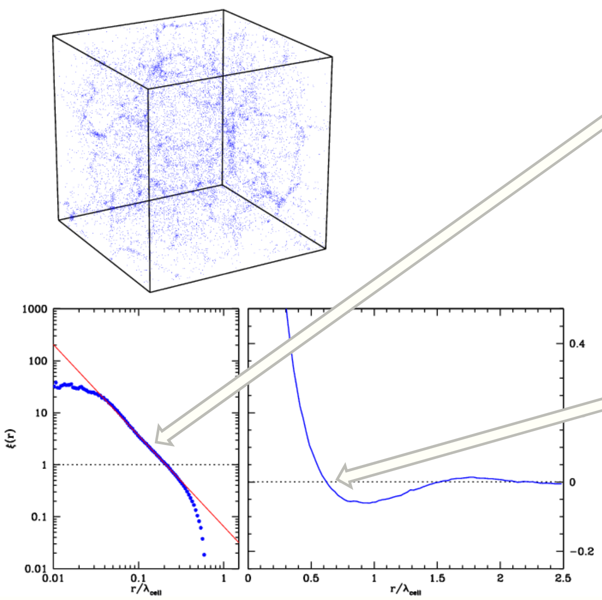

$$\xi_{cc}(r) = \left(\frac{r_o}{r}\right)^{\gamma}$$

$$\xi(r_o) = 1 .$$

Clustering length/
"Correlation" length

Coherence length

$$\xi(r_a) = 0$$

Correlation Function Estimators

Minimal Estimator

$$\hat{\xi}_{\min}(r) = \frac{V(W)}{NN_{in}} \sum_{i=1}^{N_{in}} \frac{n_i(r)}{V_{sh}} - 1$$

For galaxies close to the boundary the number of neighbours is Underestimated. One way to overcome this problem is to consider as centers for counting neighbours only galaxies lying within an inner window W_{in}

V_{sh} is the volume of the shell of width dr

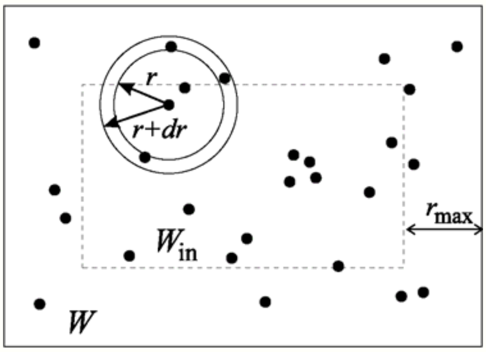

Edge-Corrected Estimator

$$\hat{\xi}_{edge}(r) = \frac{V(W)}{N^2} \sum_{i=1}^{N_{in}} \frac{n_i(r)}{V_i} - 1$$

$N_i(r)$: number of neighours at distance in the interval [r,r+dr] from galaxy I

V_i: volume of the intersection of the shell with W

W: when W a cube, an analytic expression for V_i can be found in Baddely et al. (1993).

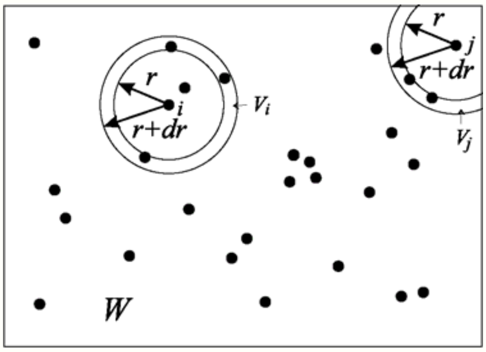

Estimators Redshift Surveys

- In redshift surveys, galaxies are not sampled uniformly over the survey volume

- Depth selection:
  in magnitude-limited surveys, the sampling density decreases as function of distance

- Survey Geometry
  boundaries of survey often nontrivially defined:
  - slice surveys
  - non-uniform sky coverage
  etc.

⇩

Clustering in survey compared with sample of Poisson distributed points, following the same sampling behaviour in depth and survey geometry

Difference in clustering between
data sample (D) and Poisson sample (R)
genuine clustering

Estimators Redshift Surveys

Clustering in survey compared with sample of Poisson distributed points, following the same sampling behaviour in depth and survey geometry

Difference in clustering between
data sample (D) and Poisson sample (R)
genuine clustering

- $$\xi_{DP}(r) = \frac{n_R}{n_D}\frac{\langle DD\rangle}{\langle DR\rangle} - 1$$ Davis-Peebles (1983)
- $$\xi_{Ham}(r) = \frac{\langle DD\rangle\langle RR\rangle}{\langle DR\rangle^2} - 1$$ Hamilton (1993)
- $$\xi_{LS}(r) = 1 + \left(\frac{n_R}{n_D}\right)^2 \frac{\langle DD\rangle}{\langle RR\rangle} - 2\,\frac{n_R}{n_D}\frac{\langle DR\rangle}{\langle RR\rangle}$$ Landy-Szalay (1993)

Angular Two-point Correlation Function

Angular Correlation Function

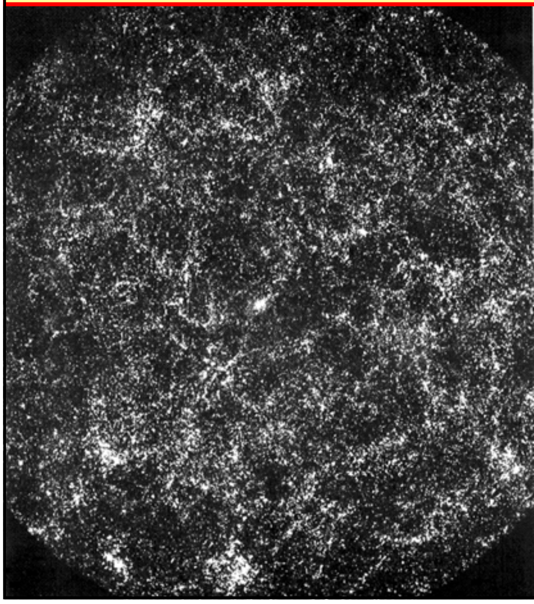

Galaxy sky distribution:

- Galaxies clustered, a projected expression of the true 3-D clustering
- Probability to find a galaxy near another galaxy higher than average (Poisson) probability
- Quantitatively expressed by 2-pt correlation function w(θ):

$$dP(\theta) = \bar{n}^2 \{1 + w(\theta)\} d\Omega_1 d\Omega_2$$

Excess probability of finding 2 gal's at angular distance θ

Angular & Spatial Clustering

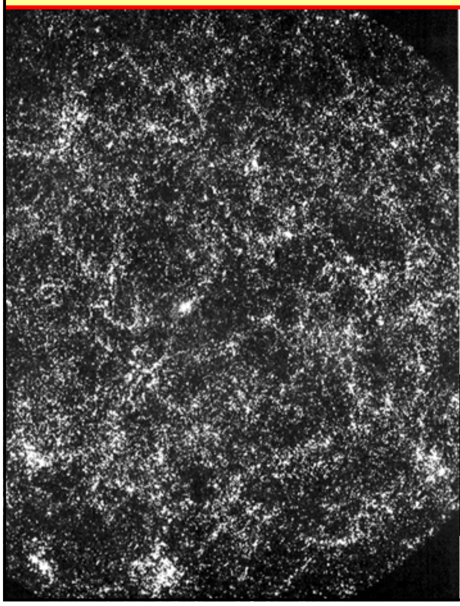

$$dP(\theta) = \bar{n}^2 \{1 + w(\theta)\} d\Omega_1 d\Omega_2$$

⇩

Two-point angular correlation function is the "projection" of $\xi(r)$

Limber's Equation:

$$w(\theta) = \frac{\iint p(\vec{x_1})\, p(\vec{x_2})\, x_1^2 x_2^2\, dx_1 dx_2\, \xi(|\vec{x_1} - \vec{x_2}|)}{\left[\int_0^\infty x^2 p(x)\, dx\right]^2}$$

p(x): survey selection function

Limber Equation

$$w(\theta) = \frac{\iint p(\vec{x_1})\, p(\vec{x_2})\, x_1^{\,2} x_2^{\,2}\, dx_1 dx_2\, \xi(|\vec{x_1} - \vec{x_2}|)}{\left[\int_0^\infty x^2 p(x)\, dx\right]^2}$$

$$\xi(r) = \left(\frac{r_0}{r}\right)^{\gamma} \longleftrightarrow w(\theta) = A\left(\frac{1}{\theta}\right)^{\gamma - 1}$$

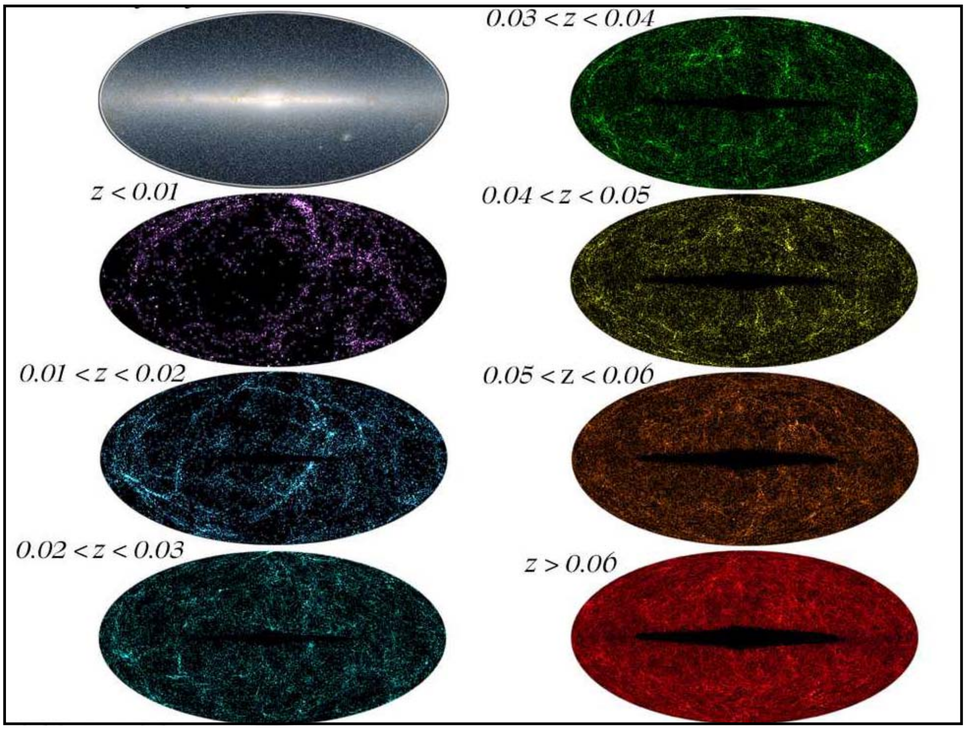

Angular Clustering Scaling

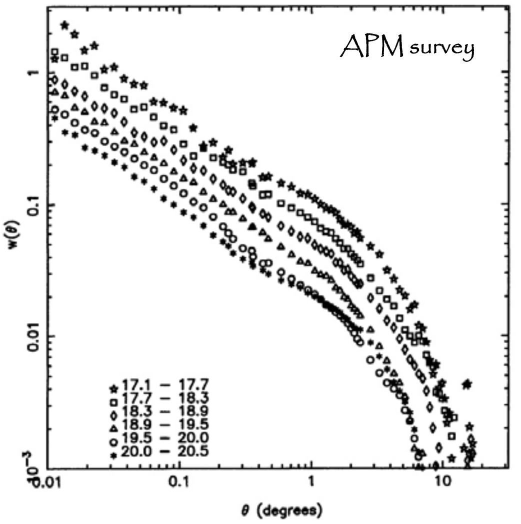

Two-point correlation function:

- small angles: power-law

$$w(\theta) = \left(\frac{\theta_0}{\theta}\right)^{\gamma}$$

$$\gamma \approx 0.8$$

- large angles → 0

  ie. to homogeneity

Angular Clustering Scaling

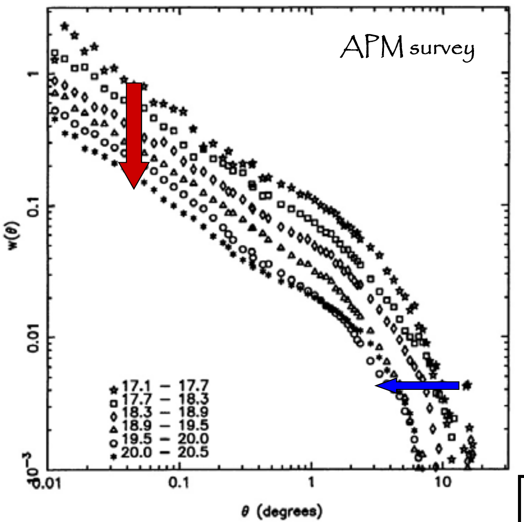

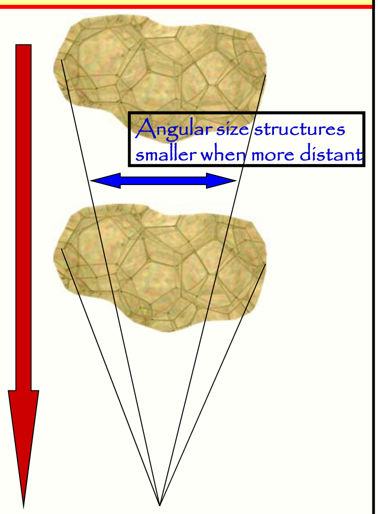

Projection of more layers leads to decreasing amplitude w(θ)

Angular Clustering Scaling

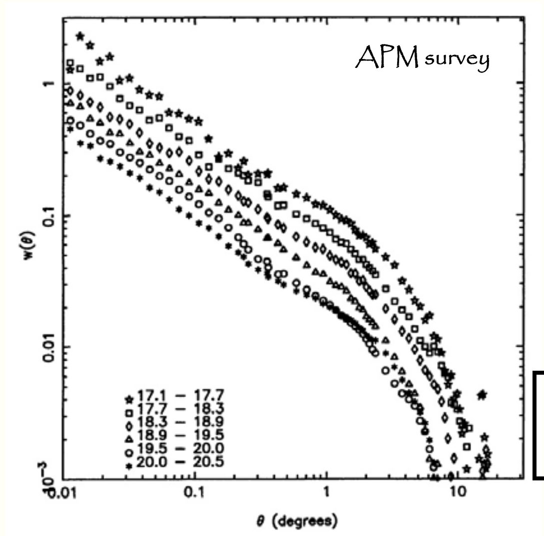

Angular size structures smaller when more distant

Projection of more layers leads to decreasing amplitude w(θ)

$$w(\theta, D_*) = \frac{1}{D_*} w(\theta D_*)$$

Angular Clustering Scaling

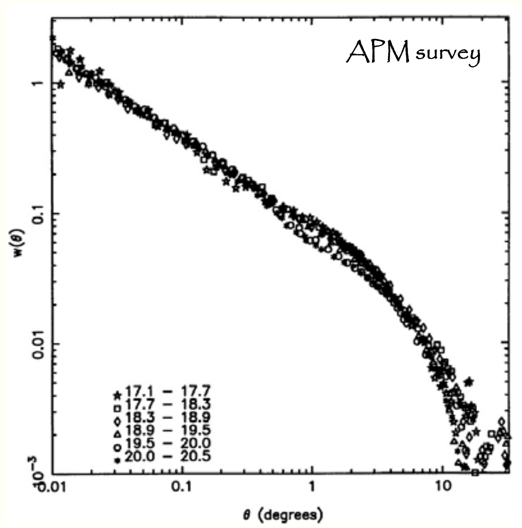

Angular size structures smaller when more distant

Projection of more layers leads to decreasing amplitude w(θ)

$$w(\theta, D_*) = \frac{1}{D_*} w(\theta D_*)$$

Angular Clustering Scaling

The angular scaling of w(θ) is found back to even fainter magnitudes in the SDSS survey (m=22)

Clear evidence that there are no significant large structures on scales > 100-200 Mpc

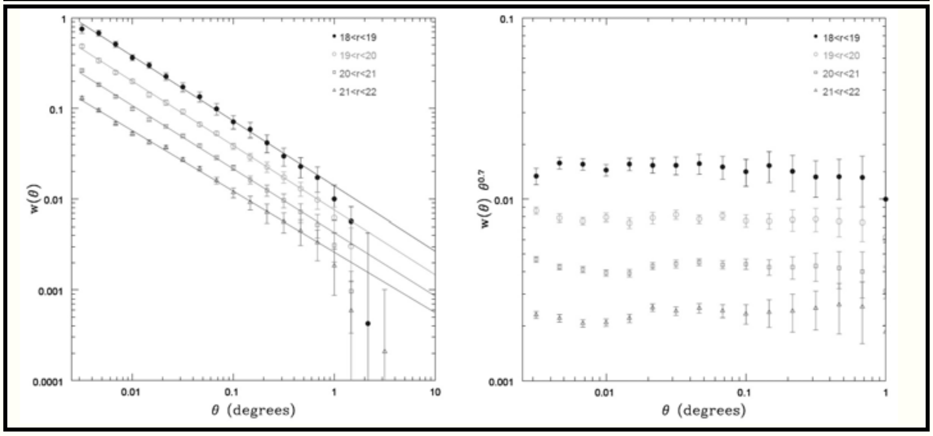

Correlation Functions:

Redshift Space

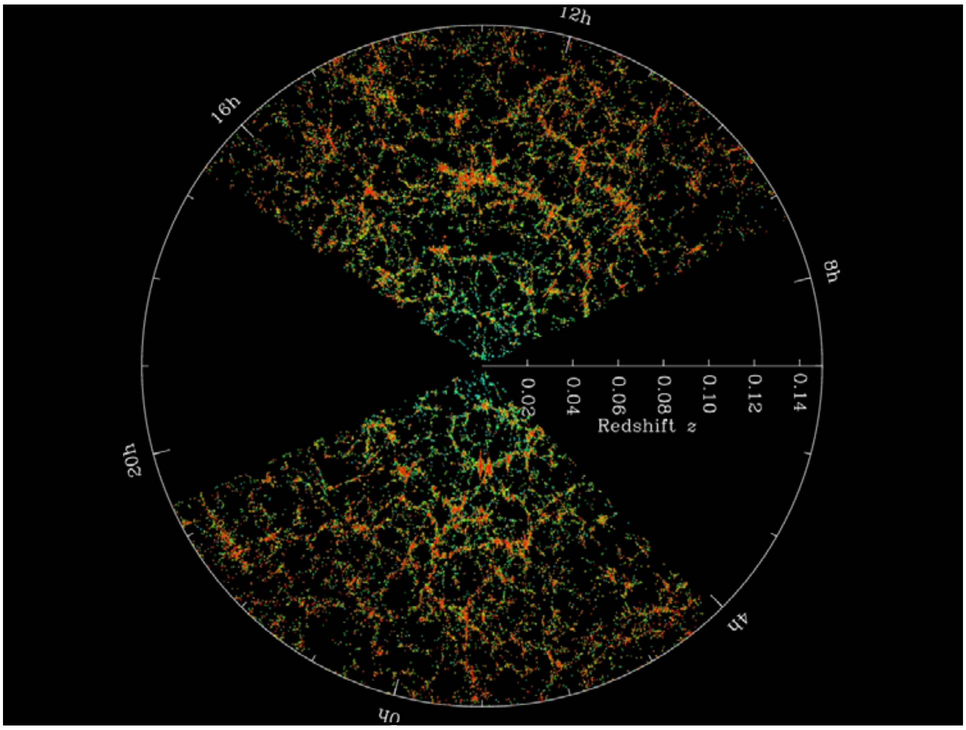
12h
16h
8h
20h
4h
0h
0.02
0.04
0.06
0.08
0.10
0.12
0.14
Redshift z

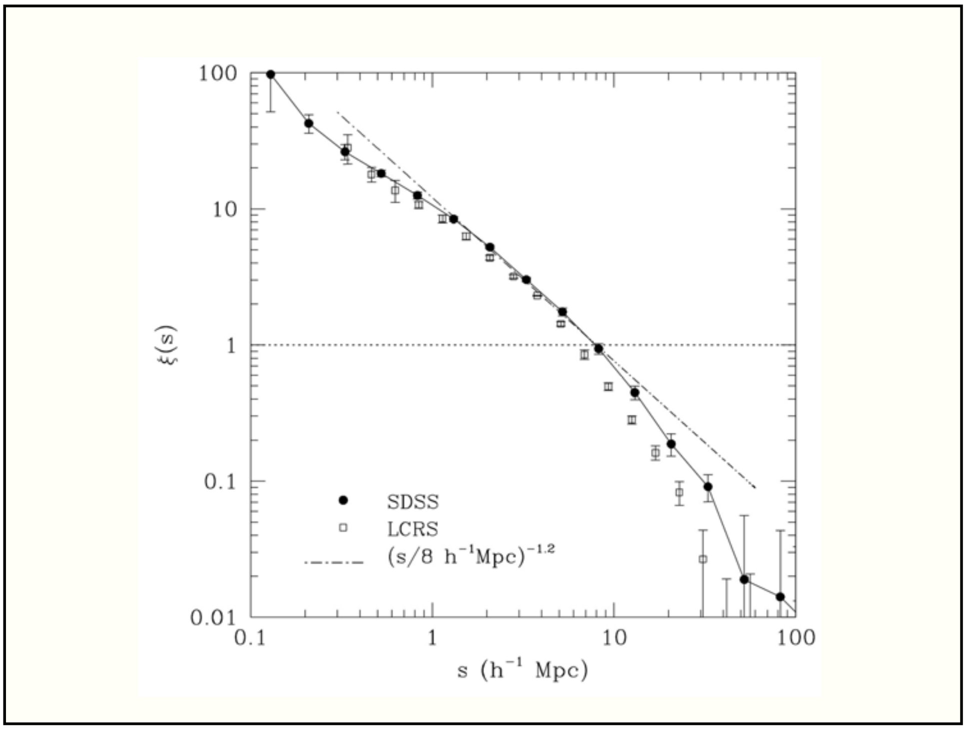
ξ(s)
s (h⁻¹ Mpc)
SDSS
LCRS
(s/8 h⁻¹Mpc)⁻¹·²
100
10
1
0.1
0.01
0.1
1
10
100

sky-redshift space 2-pt correlation function $\xi(\sigma,\pi)$

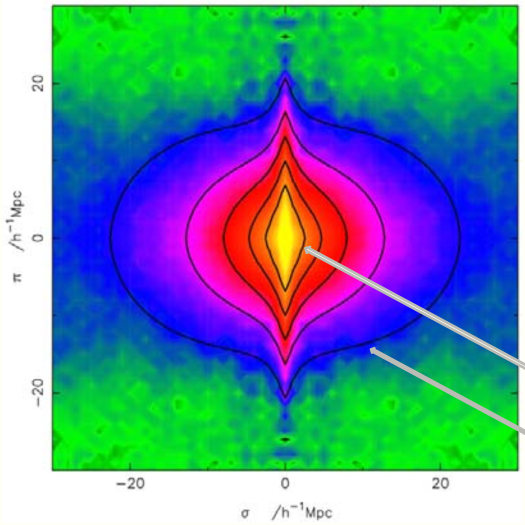

Correlation function determined in sky-redshift space:

$$\xi(\sigma,\pi)$$

sky position: $\sigma = (\alpha,\delta)$
redshift coordinate: $\pi = cz$

Close distances:
distortion due to non-linear Finger of God
Large distances:
distortions due to large-scale flows

Redshift Space Distortions Correlation Function

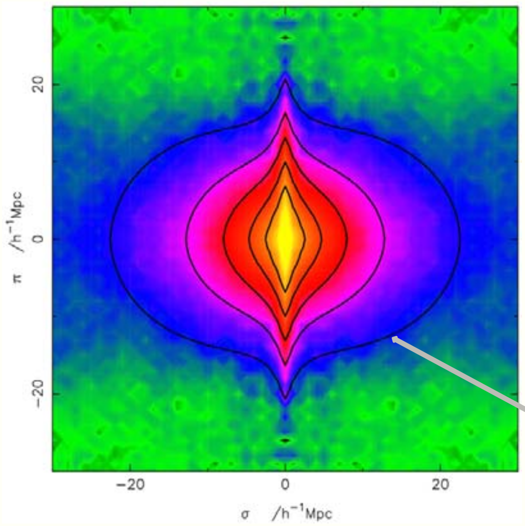

On average, $\xi_s(s)$ gets amplified wrt. $\xi_r(r)$

Linear perturbation theory (Kaiser 1987):

$$\xi_s(s) = (1+\frac{2}{3}\Omega^{0.6}+\frac{1}{5}\Omega^{1.2})\xi_r(s)$$

Large distances:
distortions due to large-scale flows

Evolution Growth Rate

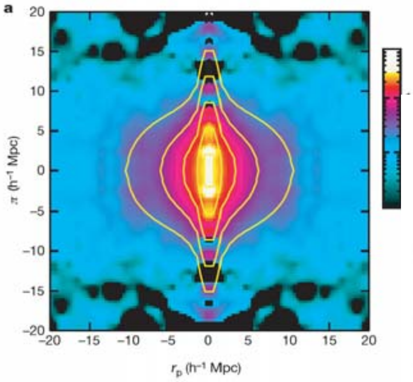

$$f(\Omega_m, \Omega_\Lambda) = \frac{a}{D}\frac{dD}{da} \approx \Omega_m^{0.55}$$

Peebles growth rate factor

Linder 2008
Guzzo et al. 2008

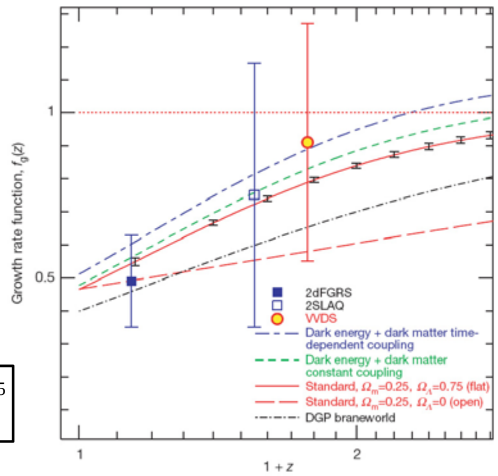

Measurement

Spatial 2pt-Correlation Function

Deprojected Spatial Correlations

2pt correlation function not an ideal power-law:

Halo Model:

Two-point correlation function combination of

1) small-scale correlations, due to galaxies inside one dark matter halo
2) large scale correlations between dark matter halos

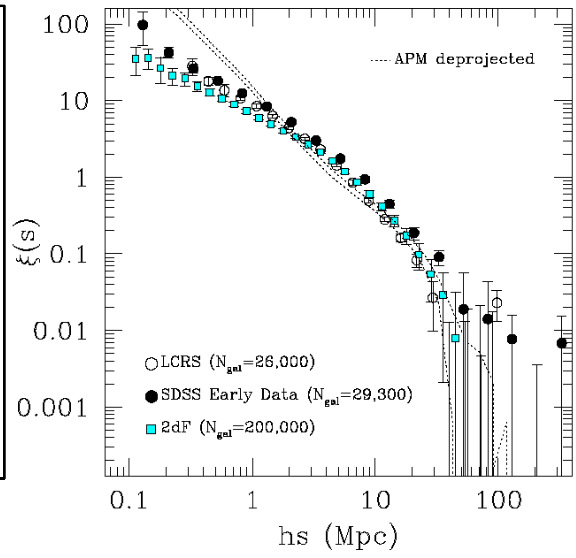

Convergence to Homogeneity

The correlation function g(r)=1+ξ(r)

Stromlo-APM, Las Campanas CfA2, ESP redshift surveys.

The fractal behavior at small scales dissapears at larger distances, providing evidence for a gradual transition to homogeneity.

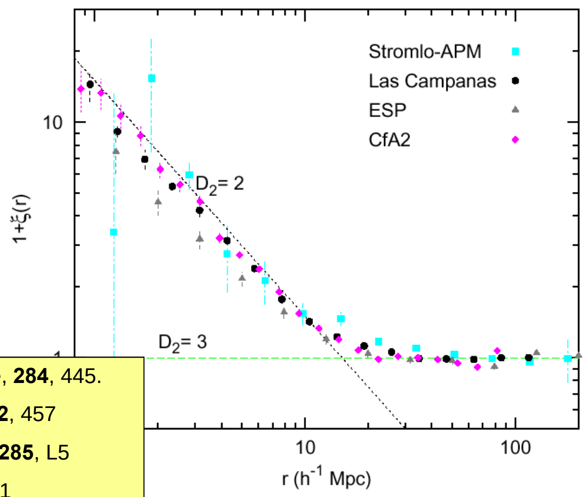

Plot from Martínez, 1999, Science, **284**, 445.

(1) Loveday *et al.*, 1995, ApJ, **442**, 457

(2) Tucker *et al.*, 1997, MNRAS, **285**, L5

(3) Guzzo *et al.*, 2000, AA, **355**, 1

Luminosity Dependence
Correlation Functions

Galaxy Luminosity Dependence

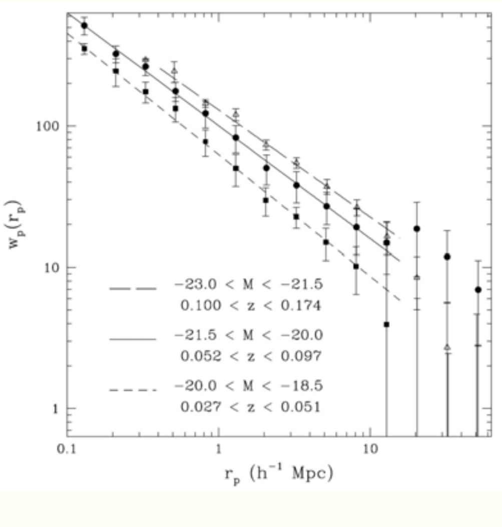

SDSS
correlation function

for galaxies in different
luminosity bins

Spatial Structure & Correlation Functions

Structural Insensitivity

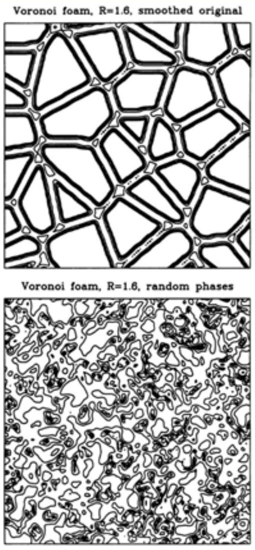

2-pt correlation function is
highly insensitive to the geometry & morphology
of weblike patterns:

compare 2 distributions with same
$\xi(r)$, cq. P(k),
but totally different phase distribution

In practice, some sensitivity in terms of distinction
Field, Filamentary, Wall-like and Cluster-dominated
distributions:

because of different fractal dimensions

Structural Sensitivity

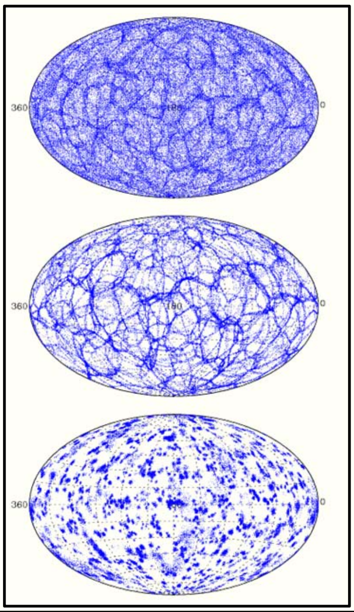

Wall-dominated

Filamentary

Cluster-like

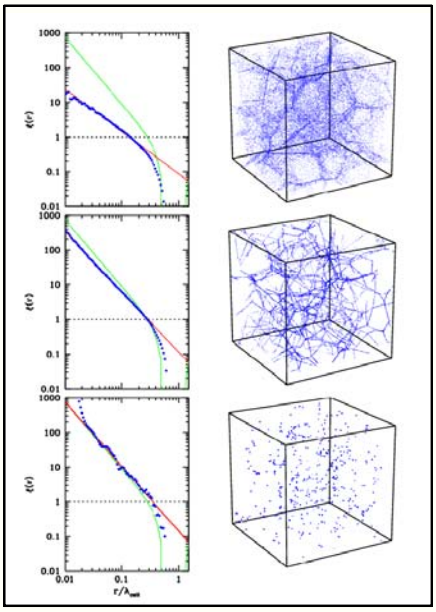

Cluster

Correlation Functions

Clusters of Galaxies

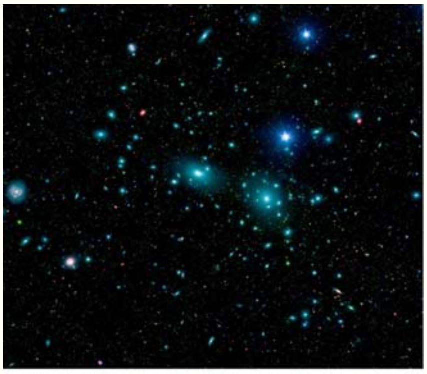

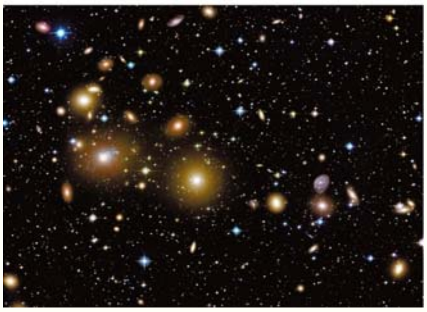

Coma Cluster

Perseus Cluster

Clustering of Clusters

Clusters cluster much more strongly than galaxies:

- clustering defines superclusters !
- also power-law 2-pt correlation fct.
- same power law slope $\gamma \sim 1.8$
- much higher correlation length r_0 :

$r_0 \sim$ 15-25 h^{-1} Mpc

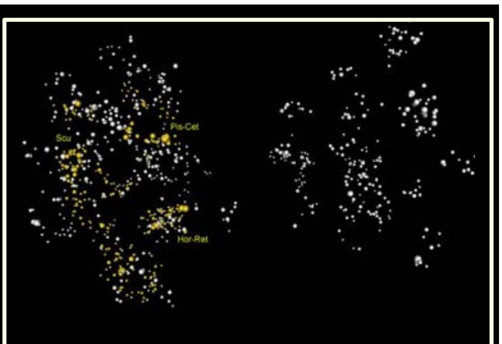

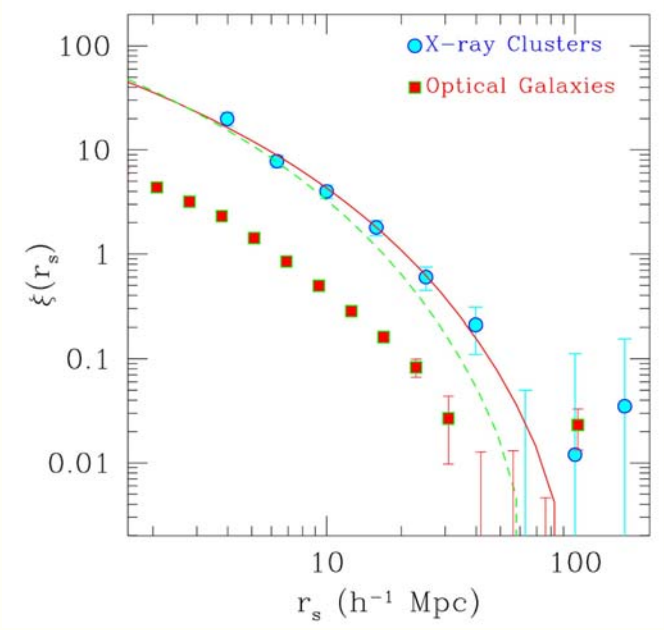

Richness-Dependent Cluster Correlations

More massive clusters are systematically more strongly clustered than lower mass ones.

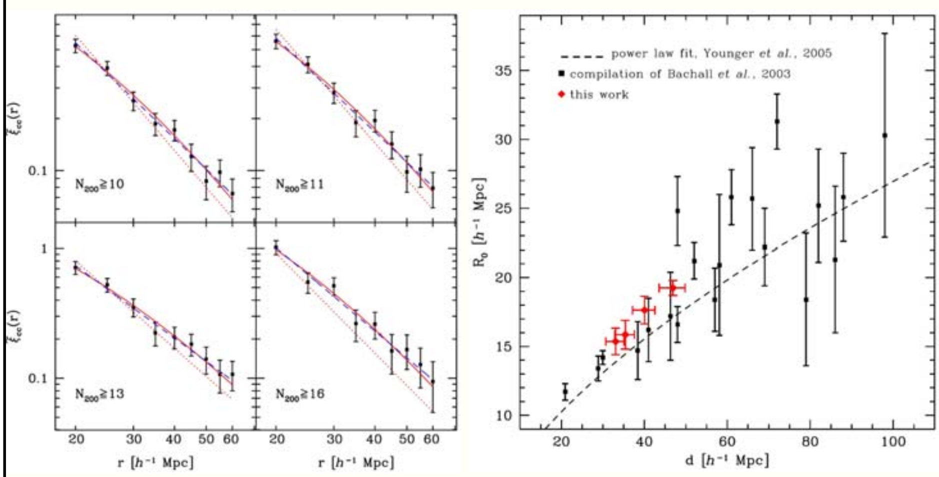

Richness-Dependent Cluster Correlations

More massive clusters are more systematically more strongly clustered than lower mass ones:

simple model:
Szalay & Schramm 1985

$$\xi_{cc}(r) = \beta \left(\frac{L(r)}{r}\right)^{\gamma}$$

$$L(R) = n^{-1/3}$$

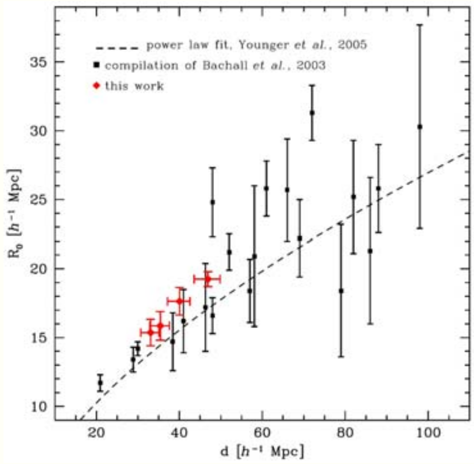

Higher Order

Correlation Functions:

N-point correlation functions

- N-point correlation function

$$\xi^{(n)}(\overrightarrow{x_1}, \overrightarrow{x_2}, \ldots, \overrightarrow{x_n})$$

- Probability function of finding an n-tuplet of galaxies in n specified volumes dV_1, dV_2, …, dV_n

$$dP(\overrightarrow{x_1}, \overrightarrow{x_2}, \ldots, \overrightarrow{x_n}) = \overline{n}^n [1 + \xi^{(n)}] dV_1 dV_2 \ldots dV_n$$

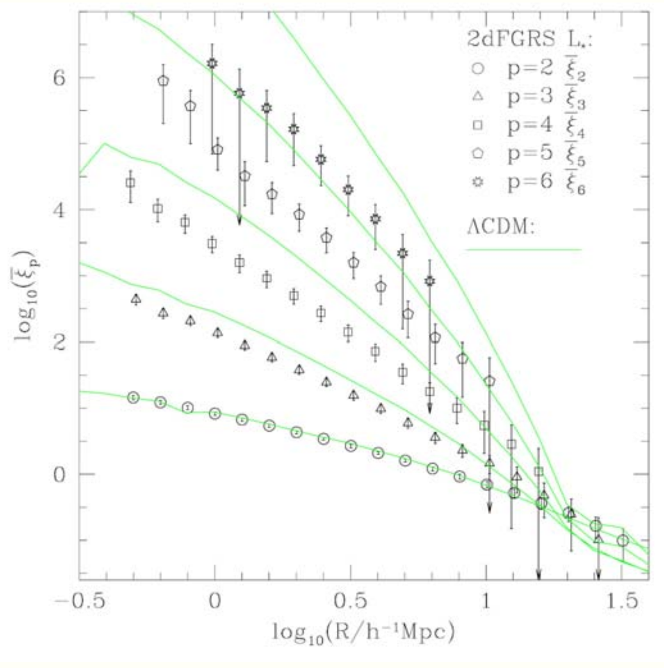

3-point correlation functions

3-point correlation function

$$dP(\vec{x}_1, \vec{x}_2, \vec{x}_3) = \bar{n}^3 [1 + \xi^{(3)}] dV_1 dV_2 dV_3$$

$$[1 + \xi^{(3)}] = \left\langle \prod_i (1 + \delta_i) \right\rangle$$

$$[1 + \xi^{(3)}] = 1 + \xi(r_{12}) + \xi(r_{13}) + \xi(r_{23}) + \zeta(\vec{r}_1, \vec{r}_2, \vec{r}_3)$$

3-point correlation functions

3-point correlation function

$$[1 + \xi^{(3)}] = 1 + \xi(r_{12}) + \xi(r_{13}) + \xi(r_{23}) + \zeta(\vec{r}_1, \vec{r}_2, \vec{r}_3)$$

reduced 3-point correlation function

$$\zeta(\vec{r}_1, \vec{r}_2, \vec{r}_3) = \langle \delta_1 \delta_2 \delta_3 \rangle$$

excess correlation over that described by the 2-pt contributions

- $\zeta \neq 0$: non-Gaussian density field
- Hierarchical ansatz (Groth & Peebles 1977)

$$\zeta(\vec{r}_1, \vec{r}_2, \vec{r}_3) = Q(\xi_{12}\xi_{23} + \xi_{23}\xi_{31} + \xi_{31}\xi_{12})$$

Power Spectrum

Power Spectrum

- Directly measuring clustering in Fourier space:
  - More intuitive physically: separating processes on different scales
  - Theoretical model predictions are made in terms of power spectrum
  - Amplitudes for different wavenumbers are statistically orthogonal

Power Spectrum P(k)

$$\delta(\mathbf{x}) = \int \frac{\mathrm{d}\mathbf{k}}{(2\pi)^3}\,\hat{\delta}(\mathbf{k})\,\mathrm{e}^{-\mathrm{i}\mathbf{k}\cdot\mathbf{x}}$$

$$(2\pi)^3 P(k_1)\,\delta_{\mathrm{D}}(\mathbf{k}_1 - \mathbf{k}_2) \equiv \langle \hat{f}(\mathbf{k}_1)\hat{f}^*(\mathbf{k}_2)\rangle$$

$$\Updownarrow$$

$$P(k) \propto \langle \hat{f}(\mathbf{k})\hat{f}^*(\mathbf{k})\rangle$$

CDM Power Spectrum P(k)

$$P_{\mathrm{CDM}}(k) \propto \frac{k^n}{[1 + 3.89q + (16.1q)^2 + (5.46q)^3 + (6.71q)^4]^{1/2}} \times \frac{[\ln(1 + 2.34q)]^2}{(2.34q)^2}$$

$$q = k/\Gamma$$

$$\Gamma = \Omega_{m,\circ} h \exp\left\{-\Omega_b - \frac{\Omega_b}{\Omega_{m,\circ}}\right\}$$

Power Spectrum P(k)

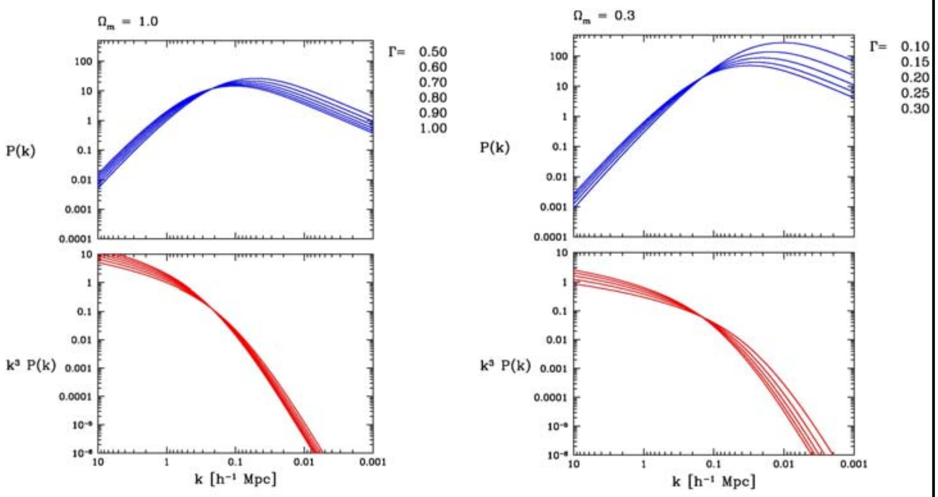

Power Spectrum - Correlation Function

$$P(k) = \int d^3 r \, \xi(\vec{r}) e^{i\vec{k}\cdot\vec{r}}$$

$$\xi(\vec{r}) = \int \frac{d^3 k}{(2\pi)^3} P(k) e^{-i\vec{k}\cdot\vec{r}}$$

Isotropy: $$\xi(r) = 4\pi \int_0^\infty \frac{k^2 dk}{(2\pi)^3} P(k) \frac{\sin(kr)}{kr}$$

Delta-power $$\Delta^2(k) = \frac{1}{2\pi^2} P(k) k^2$$

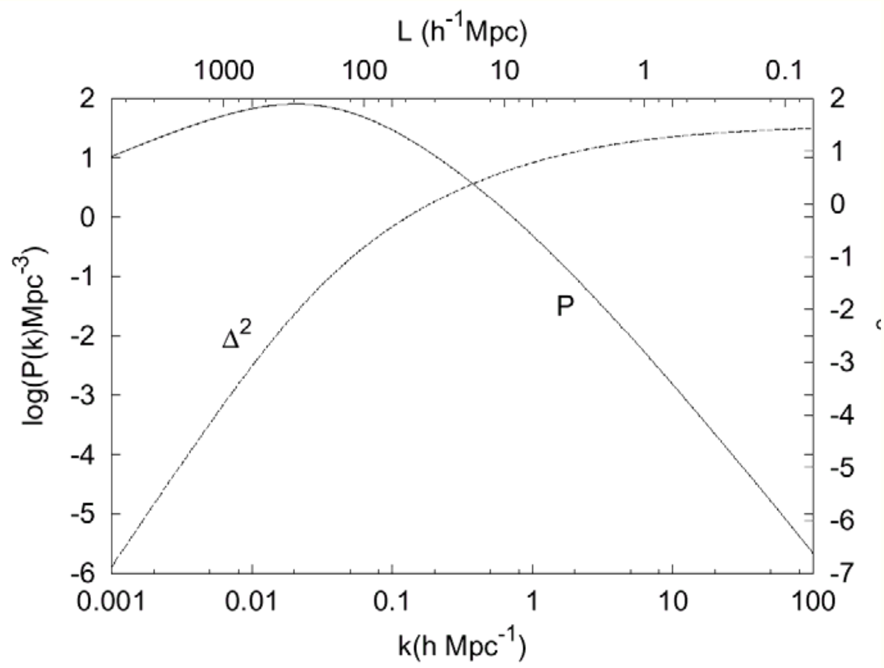

Power Spectrum Estimators

- Direct estimator
- Pixelization and maximum likelihood
- Karhunen-Loèwe (signal-to-noise) transform
- Quadratic compression
- Bayesian
- Multiresolution decomposition

Tegmark, Hamilton, Strauss, Vogeley, and Szalay, (1998), Measuring the galaxy power spectrum with future redshift surveys, ApJ, **499**, 555

Karhunen-Loeve

Decomposition in series of orthogonal
signal-noise eigenfunctions

Vogeley & Szalay 1995

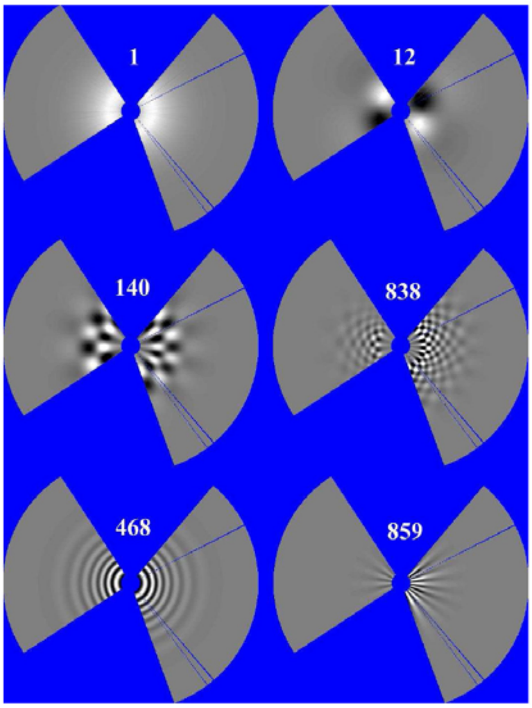

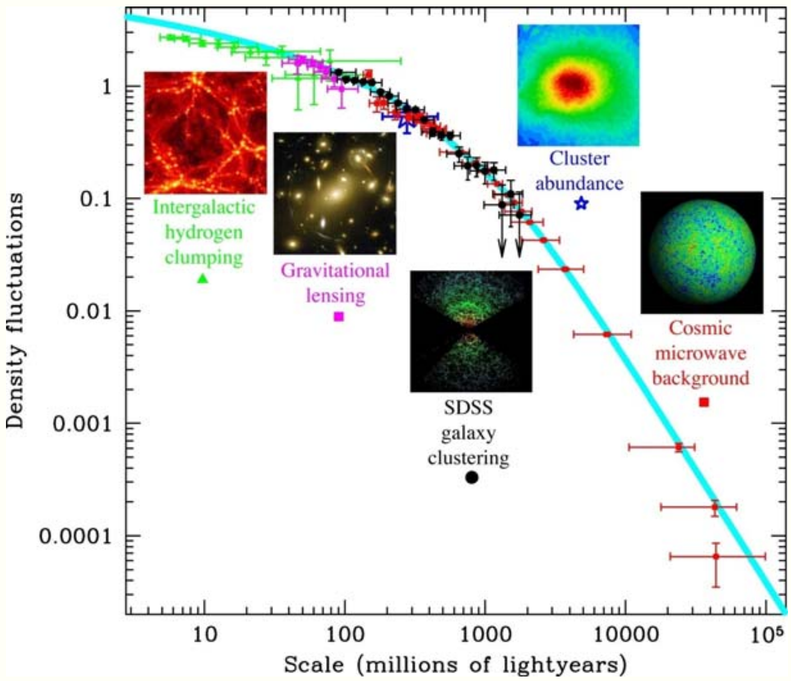

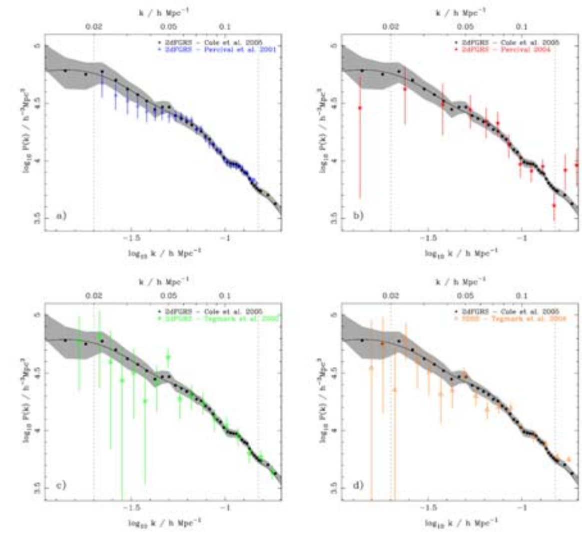

Figure 16. The redshift-space power spectrum calculated in this paper (solid circles with 1σ errors shown by the shaded region) compared with other measurements of the 2dFGRS power-spectrum shape by (a) Percival et al. (2001), (b) Percival (2005), and (c) Tegmark et al. (2002). For the data with window functions, the effect of the window has been approximately corrected by multiplying by the net effect of the window on a model power spectrum with $\Omega_m h = 0.168$, $\Omega_b/\Omega_m = 0.0$, $h = 0.72$ & $n_s = 1$. A zero-baryon model was chosen in order to avoid adding features into the power spectrum. All of the data are renormalized to match the new measurements. Panel (d) shows the uncorrelated SDSS real-space $P(k)$ estimate of Tegmark et al. (2004), calculated using their 'modelling method' with no FOG compression (their Table 3). These data have been corrected for the SDSS window as described above for the 2dFGRS data. The solid line shows a model linear power spectrum with $\Omega_m h = 0.168$, $\Omega_b/\Omega_m = 0.17$, $h = 0.72$, $n_s = 1$ and normalization matched to the 2dFGRS power spectrum.

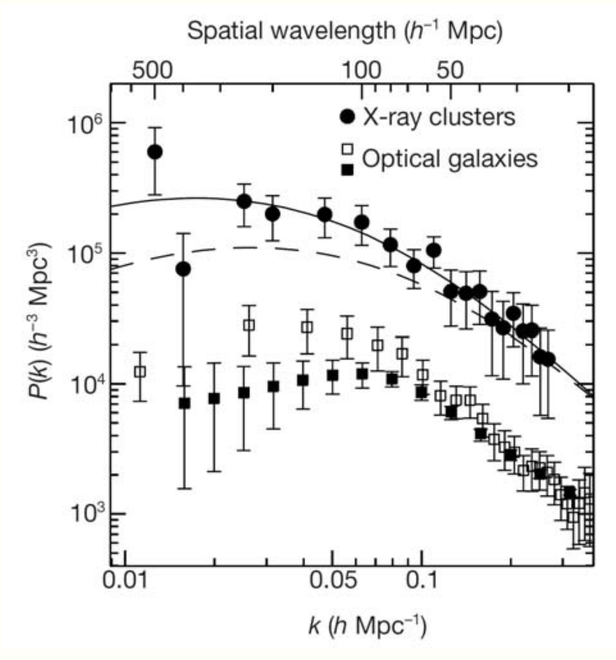

Baryonic Acoustic Oscillations

BAO

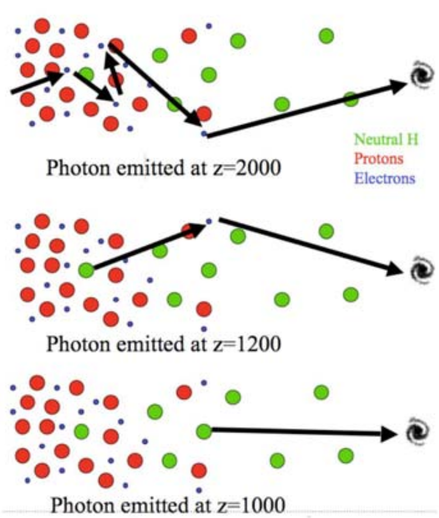

Before recombination, universe is opaque, so photons & baryons couple; interplay of gravity (DM, baryons) and photon pressure ⇒ acoustic waves propagate

At recombination, photons scatter for the last time ('surface of last scattering')

After recombination, the universe is transparent, so photons can stream freely ⇒ acoustic waves frozen

BAO

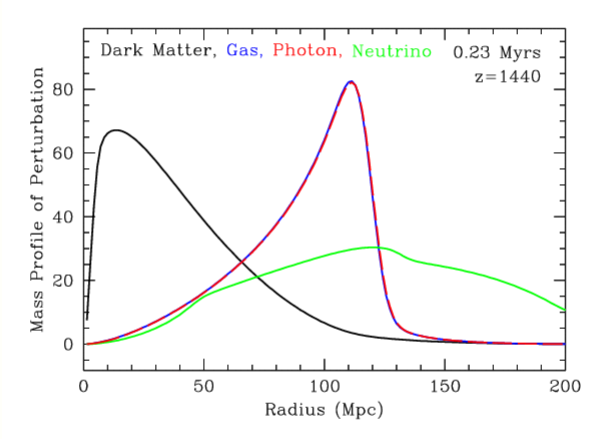
Dark Matter, Gas, Photon, Neutrino
0.23 Myrs
z=1440
Mass Profile of Perturbation
Radius (Mpc)
0
20
40
60
80
50
100
150
200

BAO

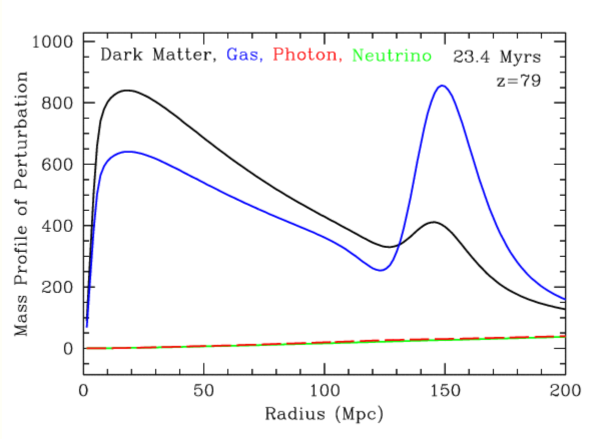
Dark Matter, Gas, Photon, Neutrino
23.4 Myrs
z=79
Mass Profile of Perturbation
Radius (Mpc)
0
200
400
600
800
1000
50
100
150
200

Measuring BAO

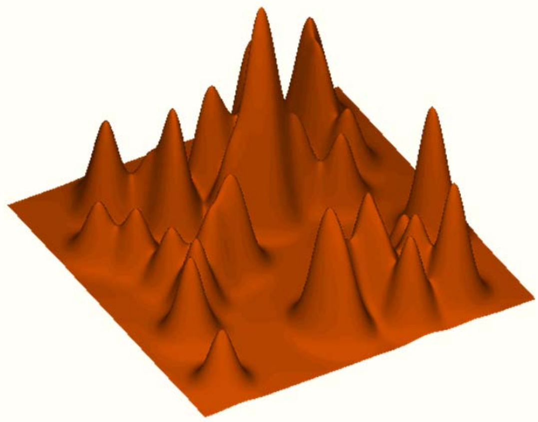

BAO as cosmological tools

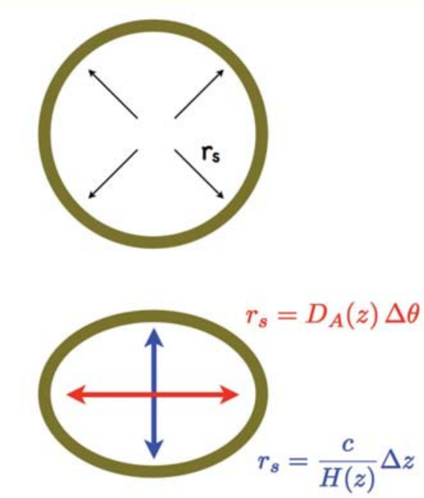

Until recombination, the sound wave travels a distance of:

$$r_s = \int_{z_{rec}}^{\infty} \frac{c_s(z)}{H(z)} dz$$

This distance can be accurately determined from the CMB power spectrum, and was found to be 147±2 Mpc.

Cosmic Constraints
LSS Clustering

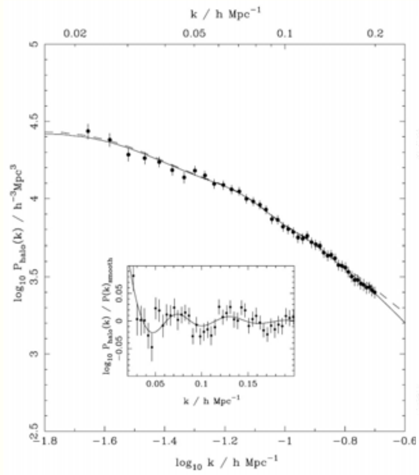

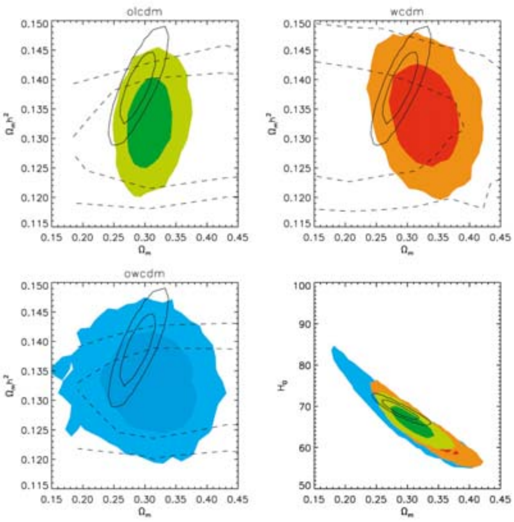

SDSS DR7 LRG sample
Clustering,   Reid et al. 2010

Topological Analysis
of the Cosmic Web

Cosmic Structure Analysis

To assess the

key aspects of the

nonlinear cosmic matter and galaxy distribution:

- multiscale character ⟷ hierarchical structure formation
- weblike network ⟷ anisotropic collapse
- volume dominance voids ⟷ asymmetry overdense vs. underdense

Many statistical measures: clustering measures (correlation functions)
density distribution functions

Topological Characteristic of network: genus statistics
Geometric Characteristics: Minkowski functionals

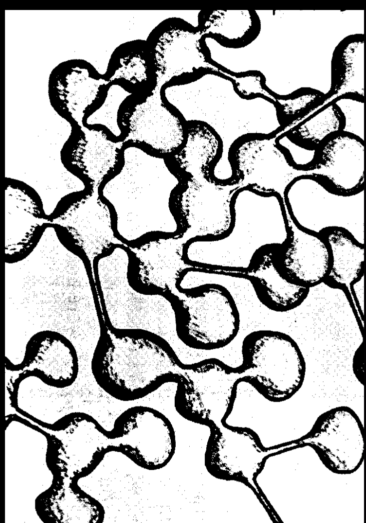

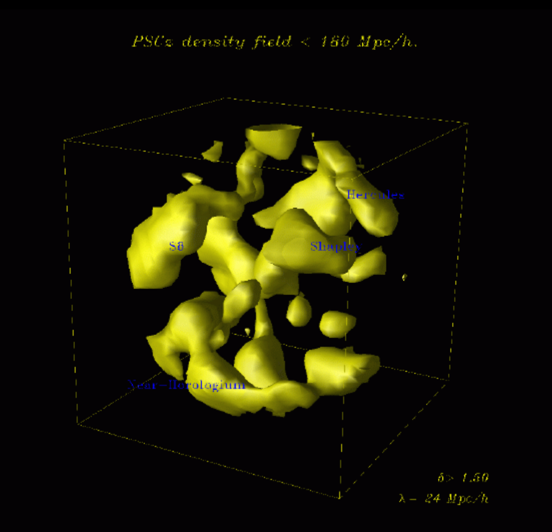

Why is the topology study useful?

1. Direct intuitive meanings

- characterize the LSS as a quantitative measure with a physical interpretation attached

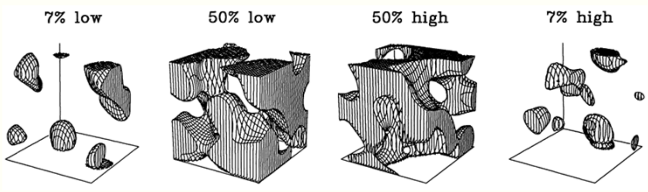

2. Easy to measure

- global genus topology from integration of local curvature:

According to the Gauss-Bonnet theorem the integrated Gaussian curvature of a surface is related with its topological genus by

$$C = \int K dA = 4\pi(1 - G)$$

Intrinsic topology

does not change by trivial change in the shape of structure
or by trivial coordinate transformation, which result in monotonic expansion/contraction, distortion, rotation ...

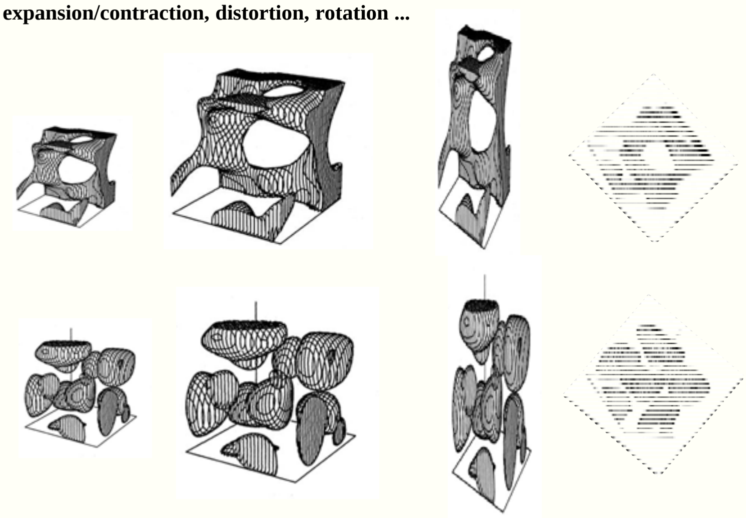

II. Introductory theory of topology statistics

Measures of intrinsic topology - **Minkowski Functionals**

3D

1. 3d genus (Euler characteristic)
2. mean curvature
3. contour surface area
4. volume fraction

→ **3d galaxy redshift survey data, 3d HI map**

2D

1. 2d genus (Euler characteristic)
2. contour length
3. area fraction

→ **CMB temp./polarization, 2d galaxy surveys**

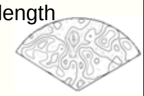

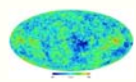

1D

1. level crossings
2. length fraction

→ **Lyα clouds, deep HI surveys, pencil beam galaxy surveys**

II. Introductory theory of topology statistics
1. Measures of intrinsic topology
2. Definitions of MFs
3. Gaussian formulae

Topological definition of the genus, $G=-V_3$

Genus = # of holes in iso-density contour surfaces - # of isolated regions

[ex. G(sphere)=-1, G(torus)=0, G(two tori)=+1]

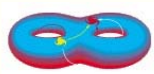

: 2 holes – 1 body = +1

The topological genus is related with the integrated Gaussian curvature of a surface by (Gauss-Bonnet theorem)

$$C = \int K dA = 4\pi(1 - G)$$

Gauss – Bonnet Theorem

For a surface with c components, the genus G specifies # handles on surface, and is related to the Euler characteristic $\chi(\partial\mathcal{M})$ via:

$$G = c - \frac{1}{2}\chi(\partial M)$$

where, according to the Gauss-Bonnet theorem, the Euler-Poincare characteristic is given by the surface integral over the Gaussian curvature

$$\chi(\partial M) = \frac{1}{2\pi}\oint\left(\frac{1}{R_1 R_2}\right) dS$$

The usefulness of Euler

The mean value of χ can be calculated analytically for Gaussian random fields (test of GRF hypothesis?)

In 3D the mean level is characterised by g>0 (a sponge)

In 2D the mean level has χ=0.

There is no 2D equivalent of a sponge!

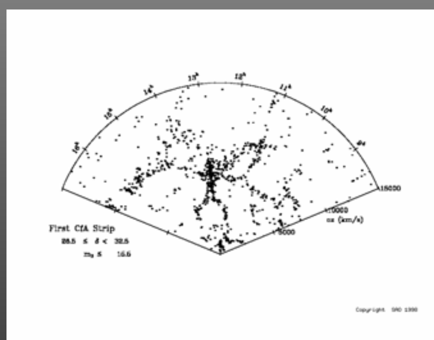

Topology

of the

Primordial Gaussian Field

Edge of the Visible Universe

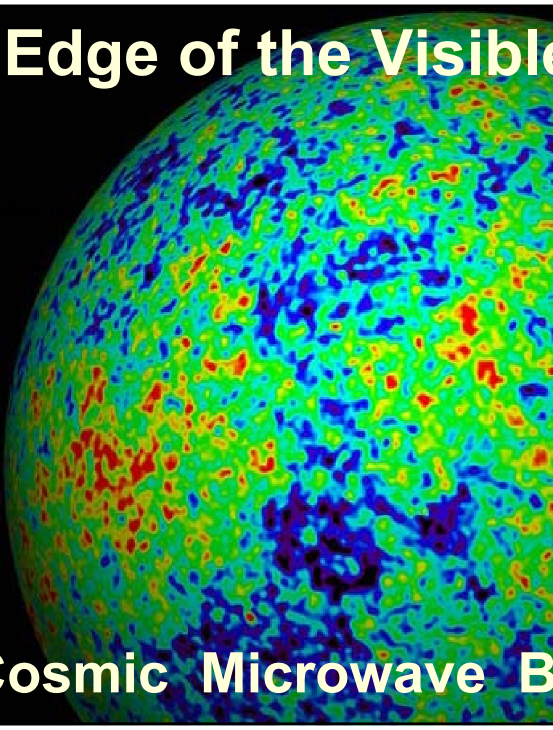

Earliest View
of our Cosmos:

the Universe
379,000 years
after the Big Bang

Perfect
Gaussian Field

Origin: Inflation,
$t = 10^{-36}$ sec

Cosmic Microwave Background

Primordial Gaussian Field

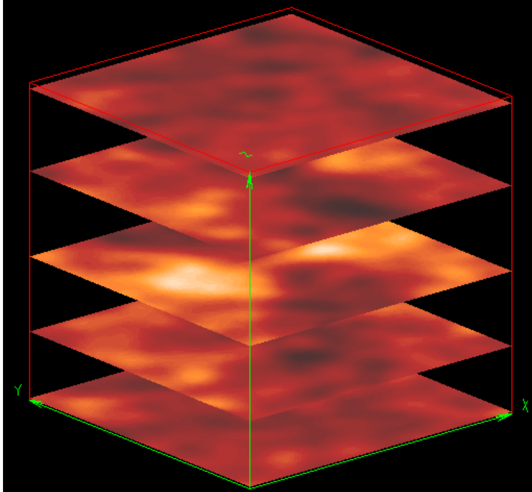

$$P_N = \frac{\exp\left[-\frac{1}{2}\sum_{i=1}^{N}\sum_{j=1}^{N} f_i \left(M^{-1}\right)_{ij} f_j\right]}{\left[(2\pi)^N (\det M)\right]^{1/2}} \prod_{k=1}^{N} df_k$$

$$\Downarrow$$

$$P_N \propto \exp\left(-\sum_i \frac{\left|\hat{f}(\vec{k}_i)\right|^2}{2P(k_i)}\right) \propto \prod_i \exp\left(-\frac{\left|\hat{f}(\vec{k}_i)\right|^2}{2P(k_i)}\right)$$

$$f(\vec{x}) = \int \frac{d\vec{k}}{(2\pi)^3} \hat{f}(\vec{k}) e^{-i\vec{k}\cdot\vec{x}}$$

$$\hat{f}(\vec{k}) = \hat{f}_r(\vec{k}) + i\,\hat{f}_i(\vec{k}) = \left|\hat{f}(\vec{k})\right| e^{i\theta(\vec{k})}$$

$$P_1\left(\left|\hat{f}(\vec{k})\right|\right) d\left|\hat{f}(\vec{k})\right| = \exp\left(-\frac{\left|\hat{f}(\vec{k})\right|^2}{2P(k)}\right) \frac{\left|\hat{f}(\vec{k})\right| d\left|\hat{f}(\vec{k})\right|}{P(k)}$$

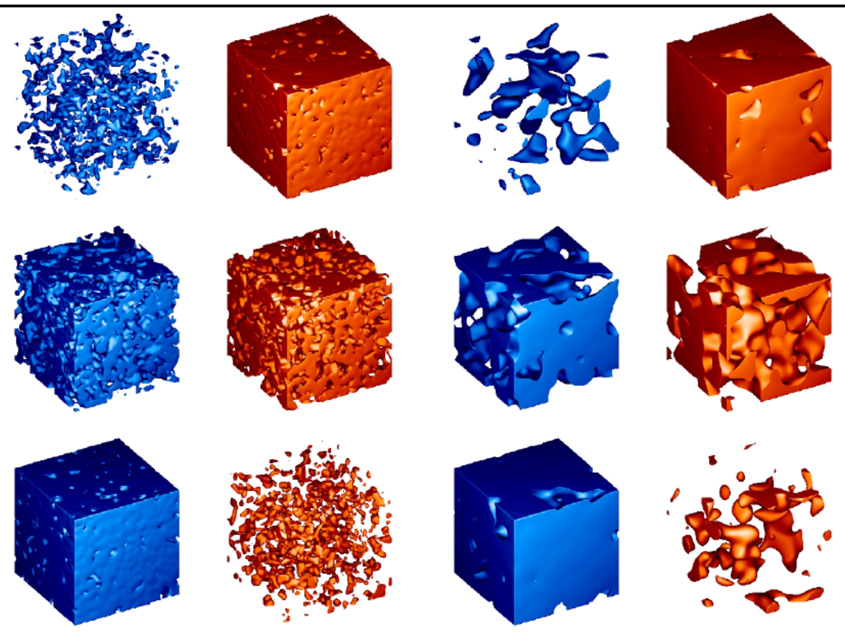

FIG. 1.— Spatial distribution of the low- (left column) and high density (right column) regions for a realization of a Gaussian random field, with comparatively little smoothing. The upper pair shows the 7% low, 93% high density regions, the middle pair stands for 50%–50%, and the lower pair shows the 93% low-density, 7% high-density case.

FIG. 2.— Spatial distribution of the low- (left column) and high density (right column) regions for a realization of a Gaussian random field, with heavy smoothing. The upper pair shows the 7% low, 93% high density regions, the middle pair stands for 50%–50%, and the lower pair shows the 93% low-density, 7% high-density case.

Gaussian Random Fields: Genus

Genus Gaussian Field, the "cosmological" way :

$$g = G - c$$

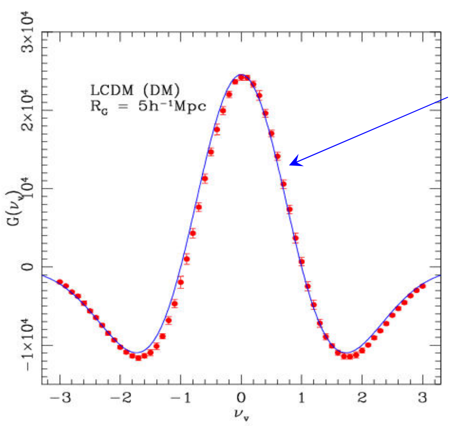

$$g(\nu) = -\frac{1}{8\pi^2}\left(\frac{\langle k^2 \rangle}{3}\right)^{3/2}\left(1-\nu^2\right)e^{-\nu^2/2}$$

$$g(\nu) = -\beta_0(\nu) + \beta_1(\nu) - \beta_2(\nu)$$

Topology

of

non-Gaussian Fields

Analytic formulae for the genus in weakly nonlinear regime due to gravitational evolution are known too (Matsubara 1994). So the non-Gaussianity due to non-linear gravitational evolution can be separated, and the primordial topology can be better explored.

$G=-V_3$

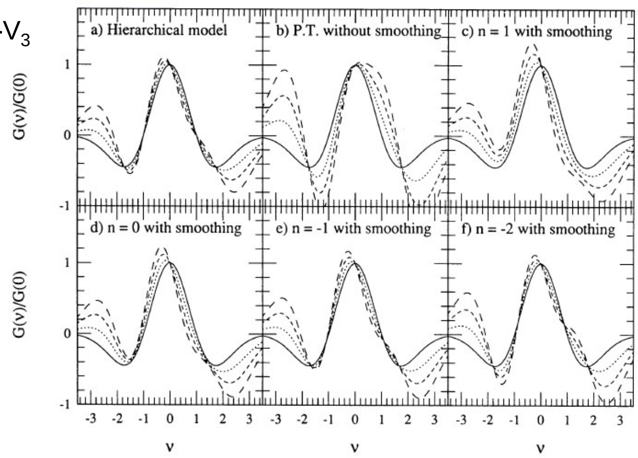

Moore et al. (1992): The topology of the QDOT IRAS redshift survey

The amplitude of the genus curves on large (21Mpc/h) scales is inconsistent with the predictions of a constant-bias SCDM model, and the shape of the best-fit PS from genus analysis is n=-1

* IRAS QDOT: 2163 redshifts out to $z=0.07$, randomly sampled at a rate of 1/6 from IRAS PSC (f_60μm > 0.6Jy), |b|>10

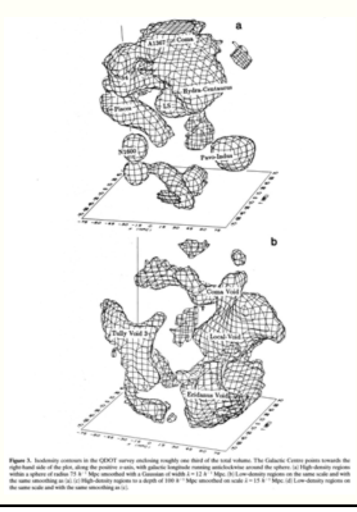

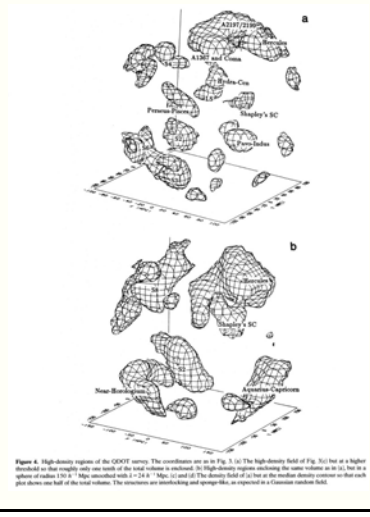

Vogeley et al. (94): Topology Analysis of the CfA Redshift Survey
Genus on R_G = 4.2 ~ 14 Mpc/h. Statistics derived from the genus curve
Amplitude drop relative to the fields with the same PS due to phase correlation on scales <10Mpc/h
→ amplitude of the genus curve is not a good measure of n.
The amplitude of the genus curves on large scales is inconsistent with the predictions of a constant bias SCDM, but consistent with a LCDM with Ωh=0.24 and Ω_Λ=0.6 and an OCDM with Ω h=0.2.
* CfA2: ~12000 galaxies with m_B < 15.5$.

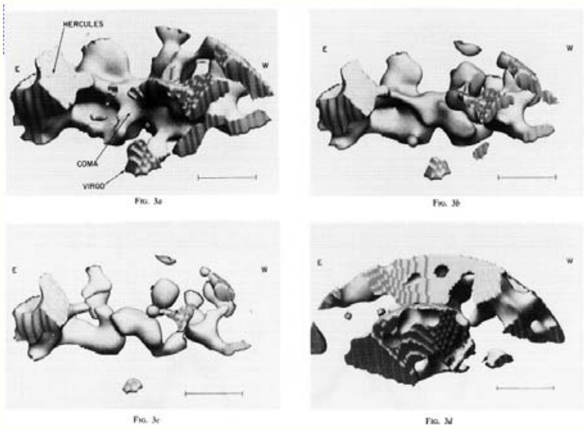

Growth of observational samples

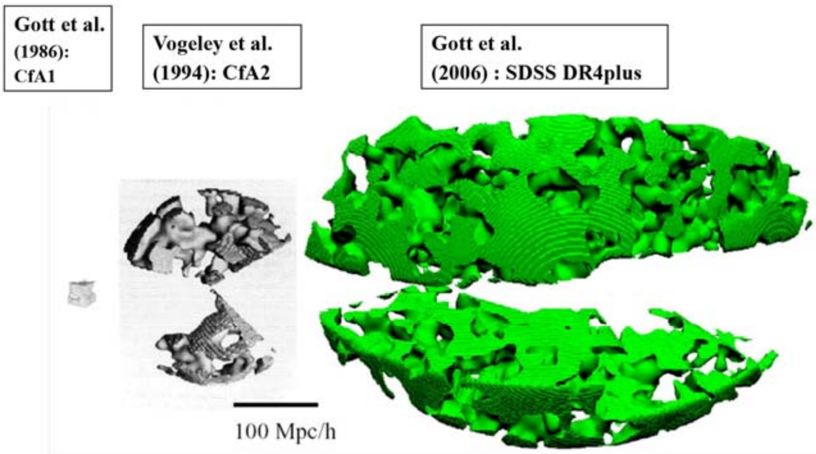

Genus Non-Gaussian Fields

Clusters | Bubbles

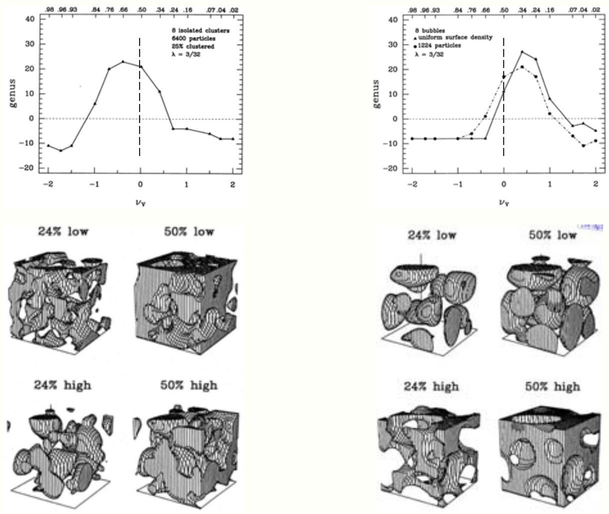

(Weinberg, Gott & Melott 1987)

Minkowski Functionals

Minkowski Functionals

- **Complete quantitative characterization of local geometry and morphology of isodensity surfaces in terms of**

Minkowski Functionals

- **Minkowski Functionals (defined by isodensity surface):**

- **Volume** $V = \int dV$

- **Surface area** $S = \oint dS$

- **Integrated mean curvature** $C = \frac{1}{2}\oint \left(\frac{1}{R_1} + \frac{1}{R_2}\right) dS$

- **Integrated Intrinsic curvature Euler Characteristic** $\chi = \frac{1}{2\pi}\oint \left(\frac{1}{R_1 R_2}\right) dS$

Minkowski Functionals: Non-Gaussianity Measure

$$V_0(\nu) = \frac{1}{2} - \frac{1}{\sqrt{2\pi}} \int_0^{\nu} \exp(-x^2/2) dx$$

$$V_1(\nu) = \frac{2}{3} \frac{\lambda}{\sqrt{2\pi}} \exp(-x^2/2)$$

$$V_2(\nu) = \frac{2}{3} \frac{\lambda^2}{\sqrt{2\pi}} \nu \exp(-x^2/2)$$

$$V_3(\nu) = \frac{\lambda^3}{\sqrt{2\pi}} (\nu^2 - 1) \exp(-x^2/2)$$

Theoretical predictions for Gaussian fields are known.

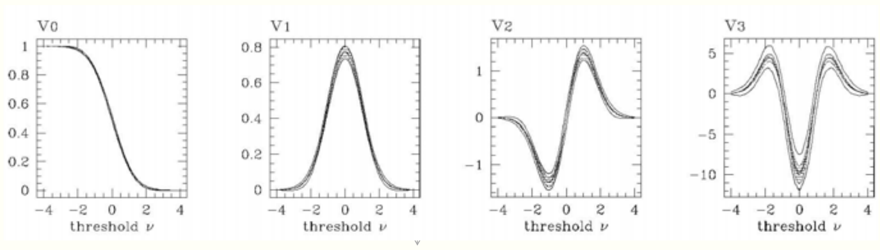

$$\lambda^3/\sqrt{2\pi} = \frac{1}{4\pi^2} \left(\frac{\langle k^2 \rangle}{3}\right)^{3/2}$$

(Schmalzing & Buchert 1997)

Minkowski functionals

In R^3 four functionals:

volume V
surface area A
integral mean curvature H
Euler-Poincare characteristic χ

These are the Minkowski Functionals

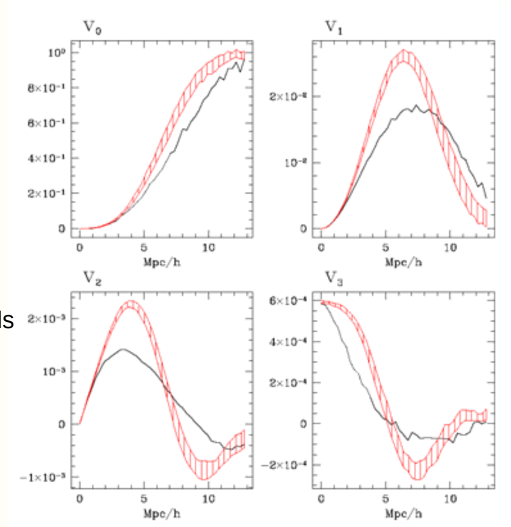

Kerscher & Martínez (1998),
Bull. Int. Statist. Inst. 57-2, 363

Homology Analysis of the Cosmic Web

Cosmic Structure Topology

- Complete quantitative characterization of homology in terms of

Betti Numbers

- Betti number β_k: - rank of homology groups Hp of manifold
  - number of k-dimensional holes of an object or shape

- 3-D object, e.g. density superlevel set:

β_0: - # independent components
β_1: - # independent tunnels
β_2: - # independent enclosed voids

Geometry & Topology

- Complete quantitative characterization of homology in terms of

Betti Numbers

- Complete quantitative characterization of local geometry in terms of

Minkowski Functionals

- Minkowski Functionals:
  - Volume
  - Surface area
  - Integrated mean curvature
  - Genus/Euler Characteristic

Genus, Euler & Betti

- Euler – Poincare formula

  Relationship between Betti Numbers & Euler Characteristic χ:

$$\chi = \sum_{k=0}^{d} (-1)^k \beta_k$$

Genus, Euler & Betti

- Euler – Poincare formula

  Relationship between Betti Numbers & Euler Characteristic χ.

3-D manifold $\mathcal{M}$:

$$\chi(M) = \beta_0 - \beta_1 + \beta_2 + \beta_3$$
$$\approx \beta_0 - \beta_1 + \beta_2$$

2-D boundary manifold $\partial\mathcal{M}$:

$$\chi(\partial M) = \beta_{0b} - \beta_{1b} + \beta_{2b}$$

Genus, Euler & Betti

- For a surface with c components, the genus G specifies # handles on surface, and is related to the Euler characteristic $\chi(\partial\mathcal{M})$ via:

$$G = c - \frac{1}{2}\chi(\partial M)$$

where, according to the Gauss-Bonnet theorem

$$\chi(\partial M) = \frac{1}{2\pi}\oint\left(\frac{1}{R_1 R_2}\right) dS$$

- **Euler characteristic 3-D manifold $\mathcal{M}$ & 2-D boundary manifold $\partial\mathcal{M}$:**

$$\chi(M) = \frac{1}{2}\chi(\partial M)$$

$$\Downarrow$$

$$\chi(\partial M) = 2(\beta_0 - \beta_1 + \beta_2)$$

Gaussian Random Fields: Betti Numbers

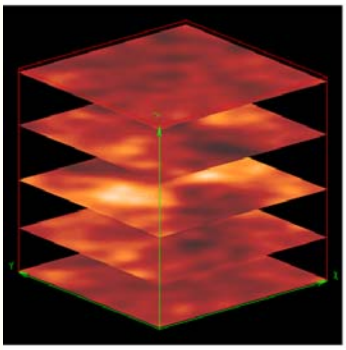

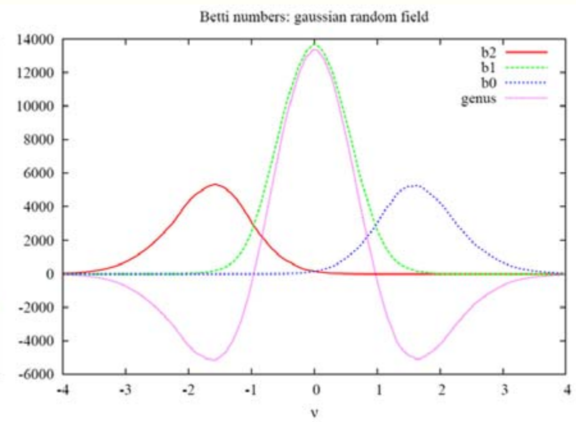

In a Gaussian field:

- # tunnels dominant at intermediate density levels, when superlevel domain spongelike
- overlap between β_0 and β_2 at ν=0, domain punctured by clumps with cavities
- # clumps/islands reaches maximum at $\nu = \sqrt{3}$, # cavities/voids at $\nu = -\sqrt{3}$

Gaussian Random Fields: Betti Numbers

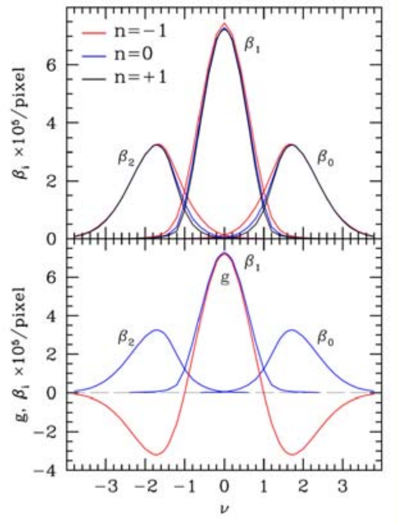

Distinct sensitivity of Betti curves on power spectrum P(k):

unlike genus (only amplitude P(k) sensitive)

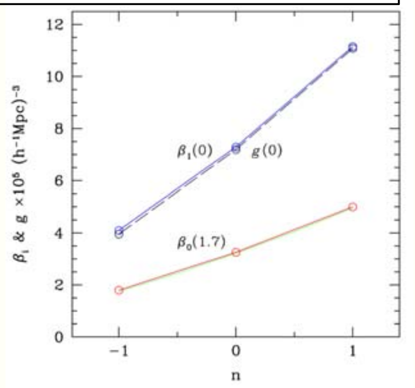

Gaussian Random Fields: Correlation Betti Numbers

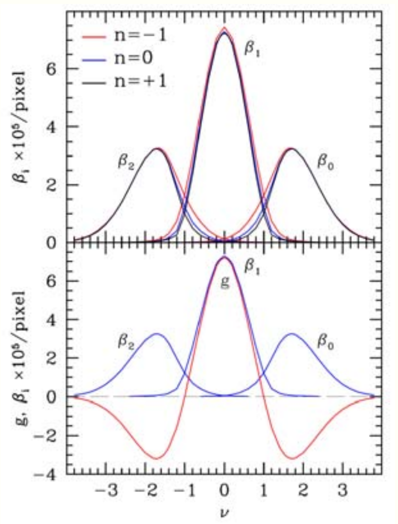

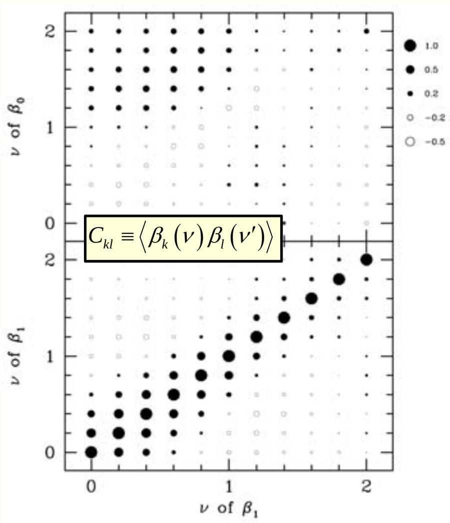

Gaussian Random Fields: Betti Numbers

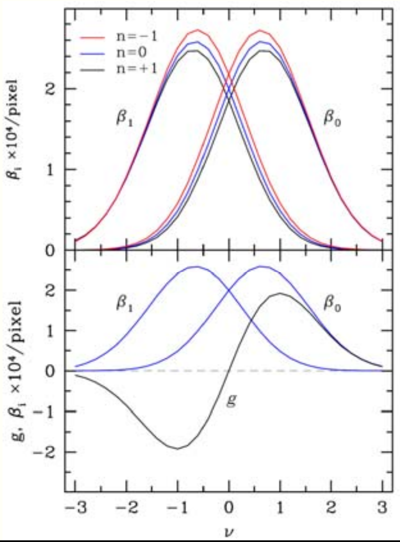

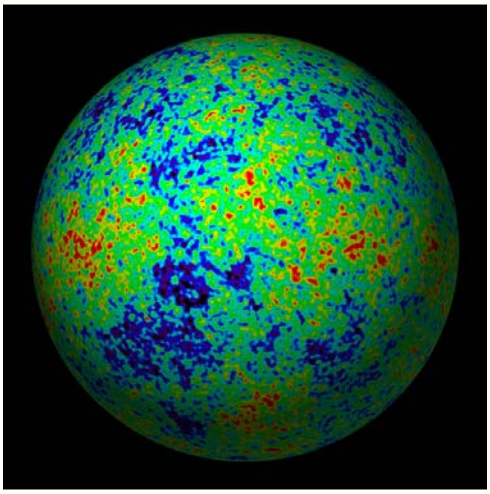

Homology

of the Cosmic Web

Homology of evolving LCDM cosmology

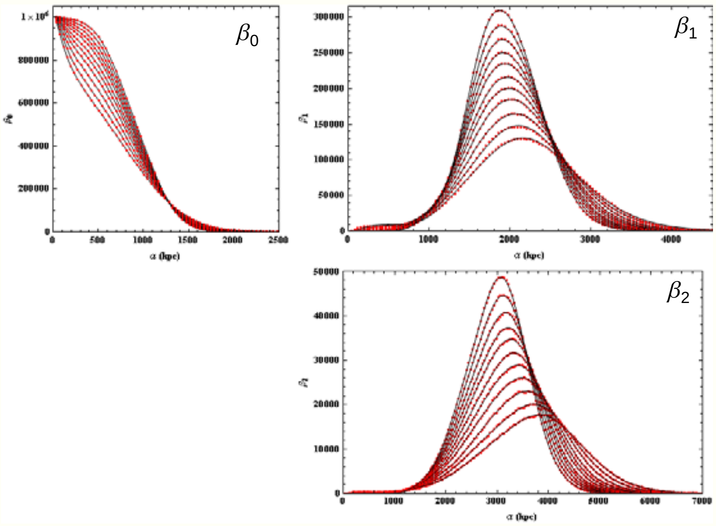

Betti$_2$:

evolving void populations

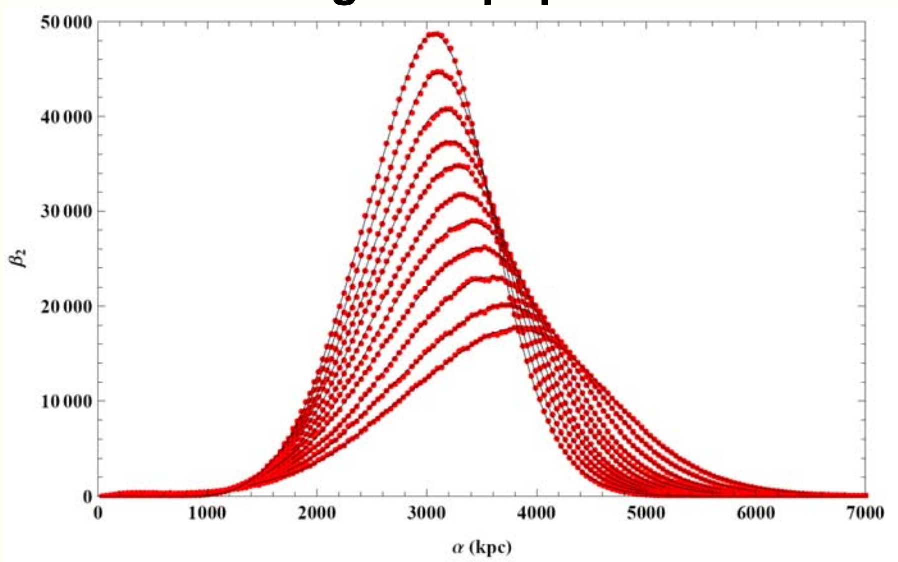

LCDM vs. SUGRA

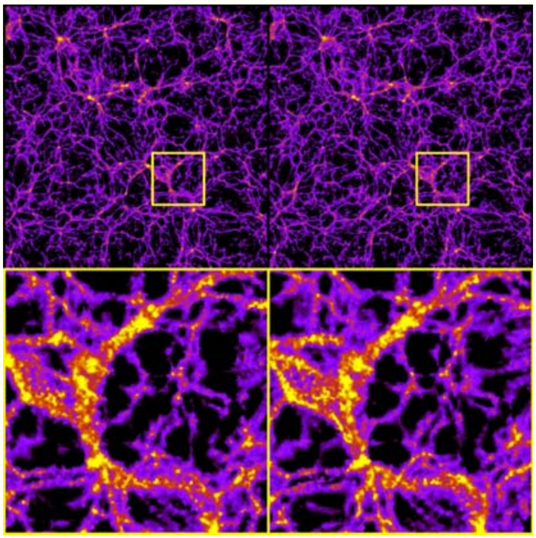

Homology

sensitivity LCDM vs. Quintessence

β_0 β_1 β_2

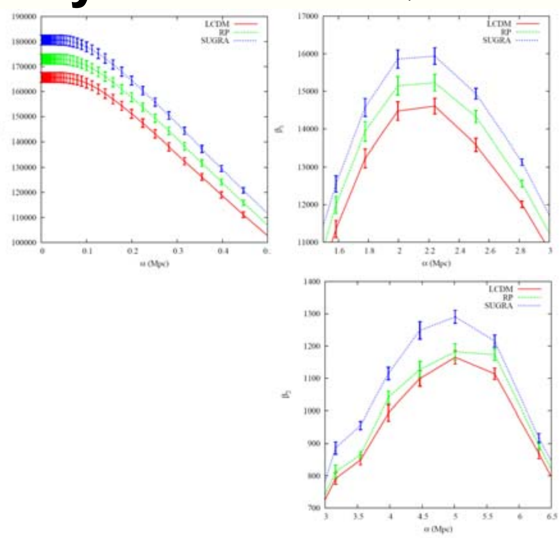

Persistence

Persistence: search for topological reality

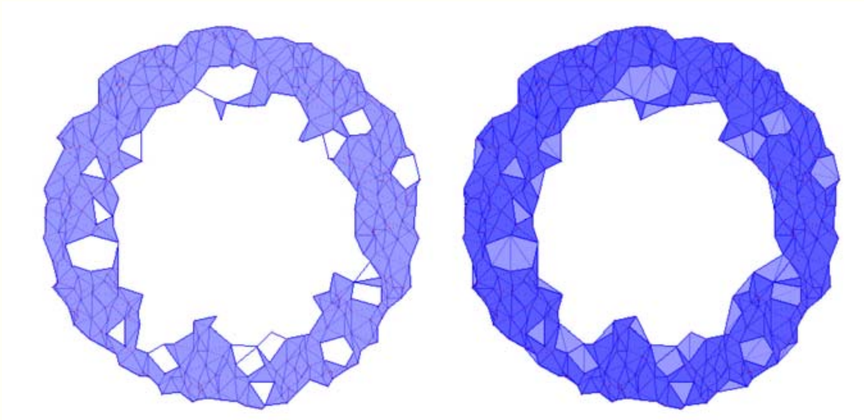

Concept introduced by Edelsbrunner:

Reality of features (eg. voids) determined on the basis of α-interval between "birth" and "death" of features

Persistent Homology

Persistent Homology describes the homological features which persist as a single parameter changes

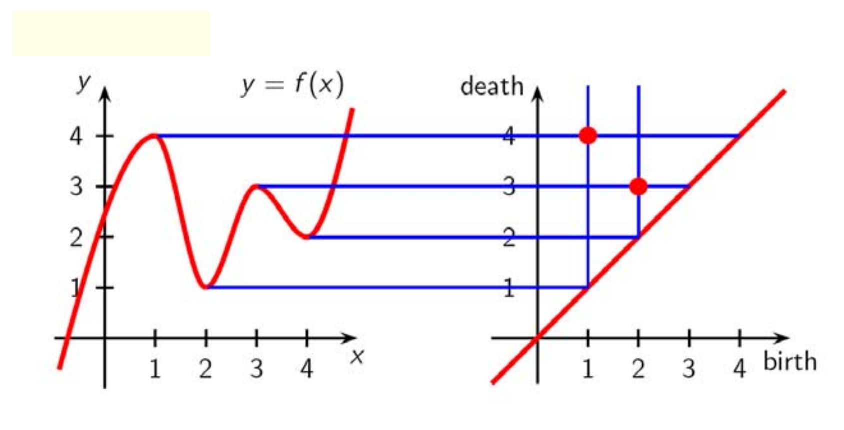

Persistent LCDM Cosmic Web

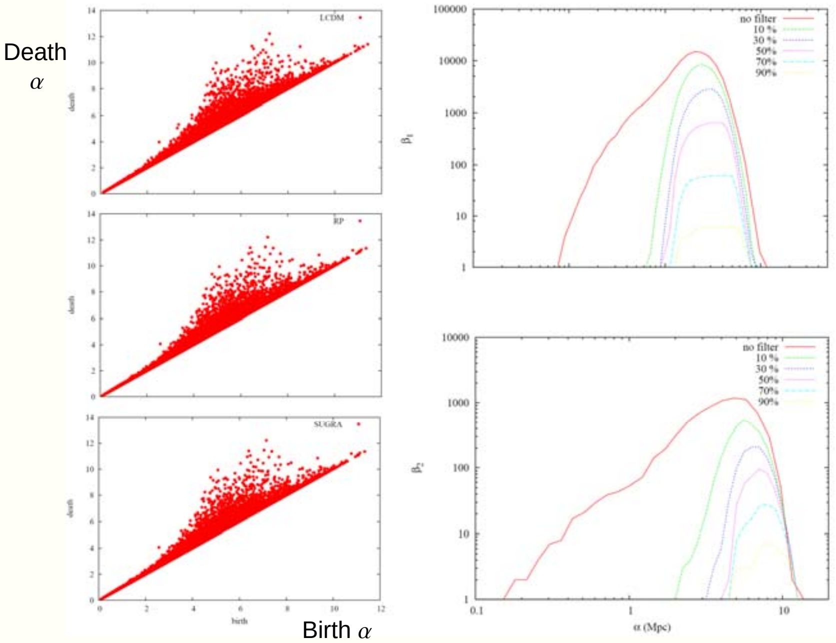

Minimal Spanning Tree

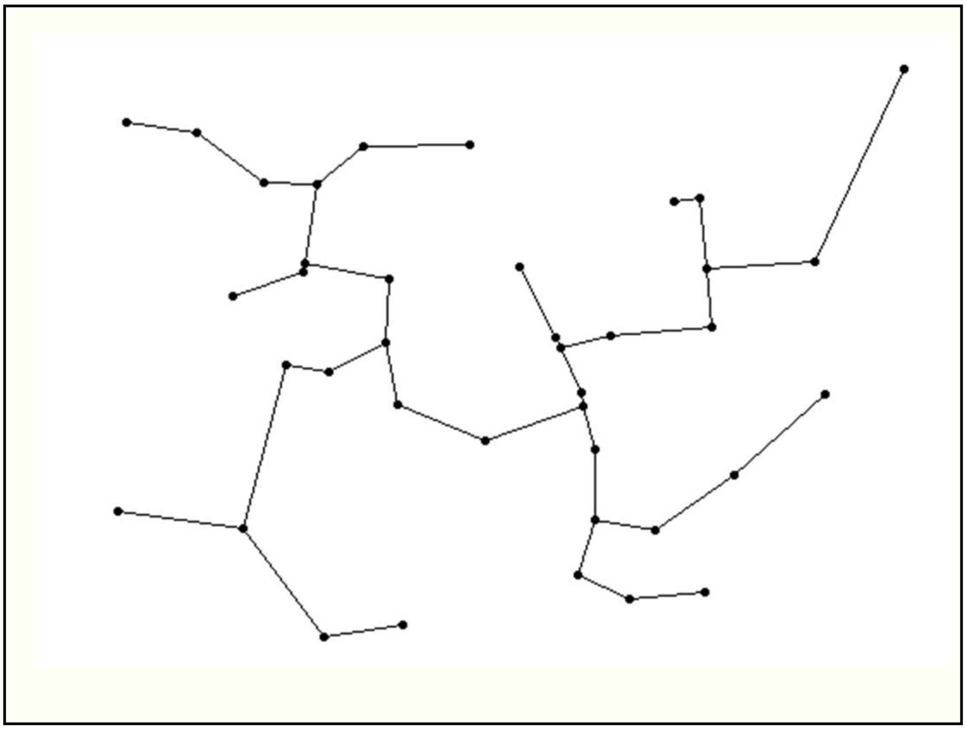

Morse Theory

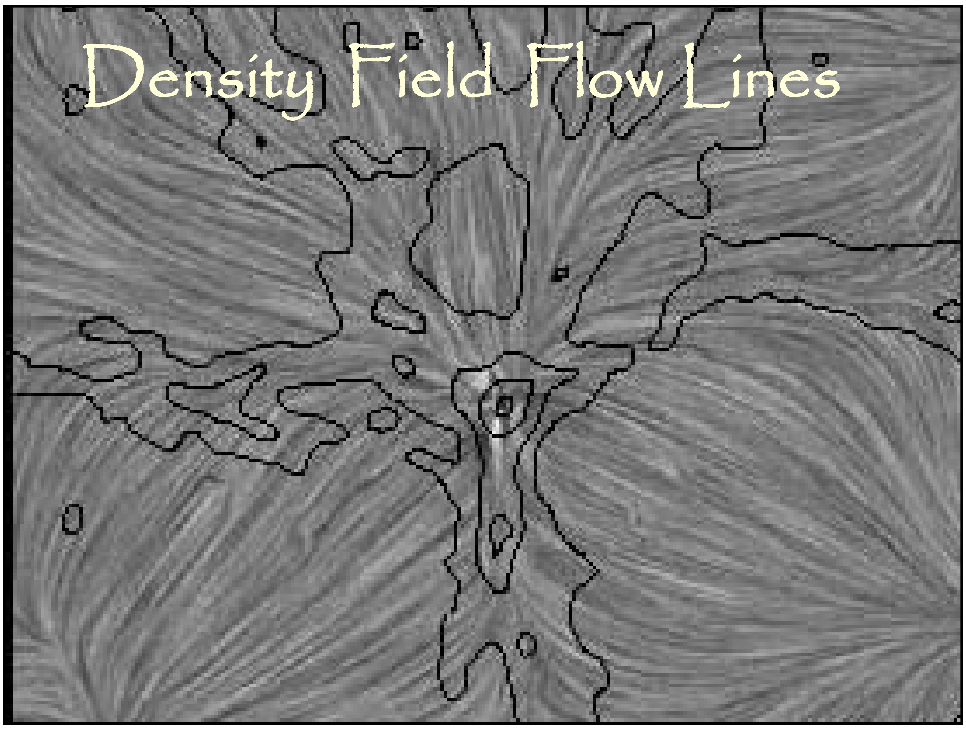

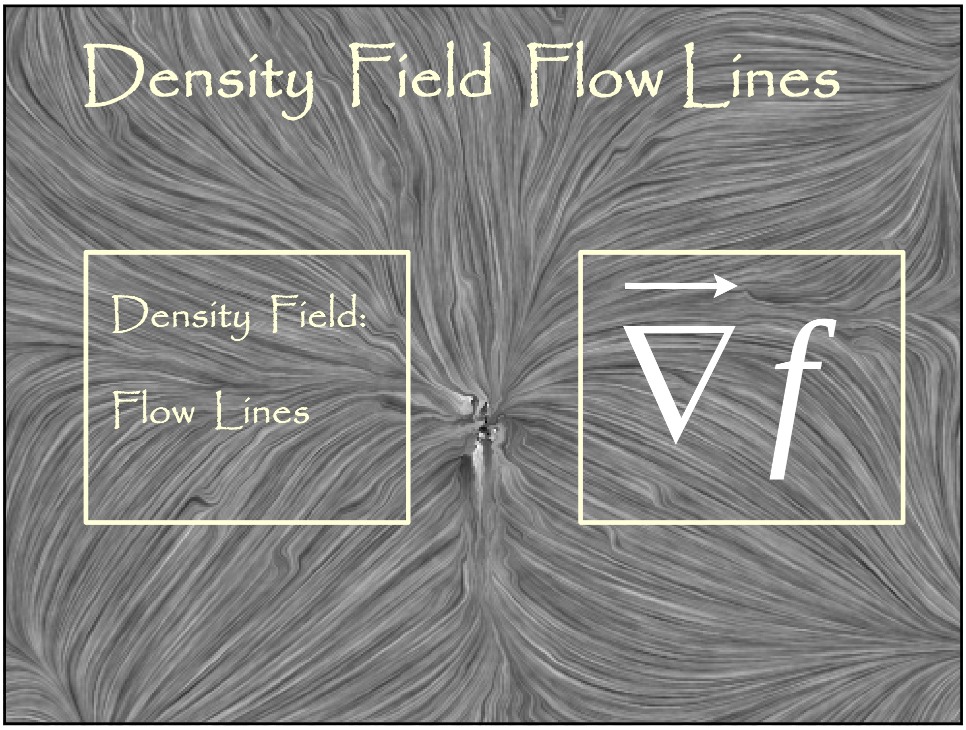
Density Field Flow Lines
Density Field:
Flow Lines
$\vec{\nabla} f$

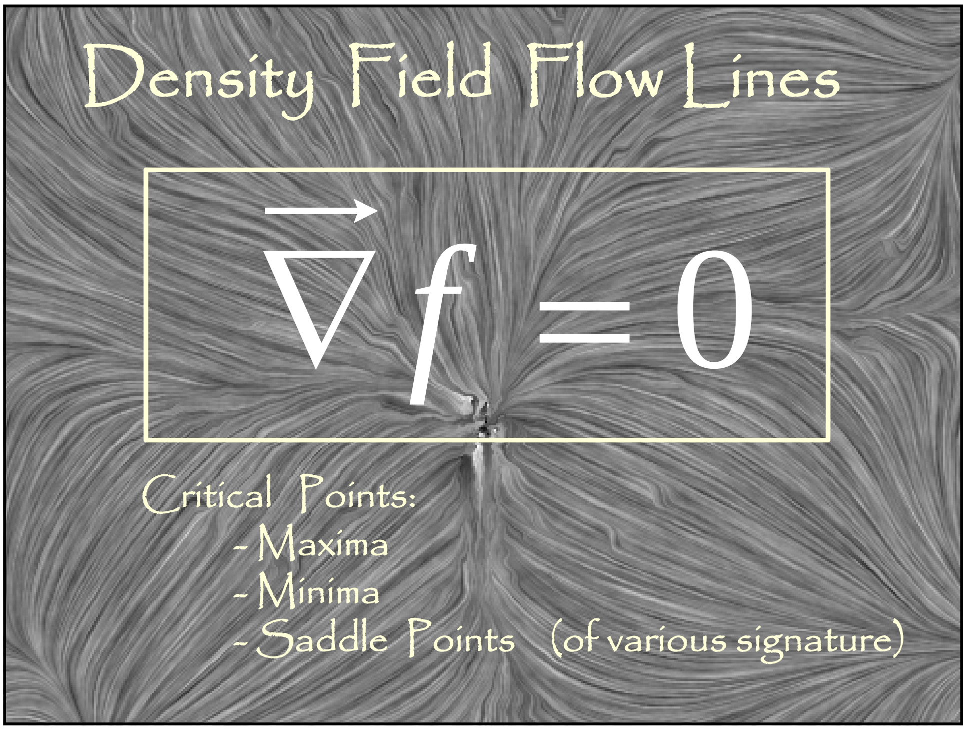
Density Field Flow Lines
$\vec{\nabla} f = 0$
Critical Points:
- Maxima
- Minima
- Saddle Points (of various signature)

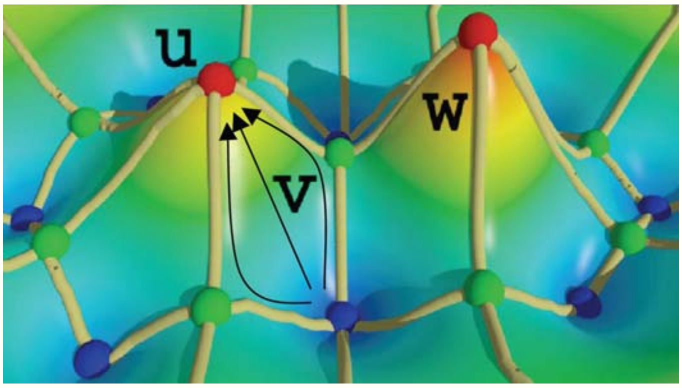

Density Field Critical Points:

Ridges:

Connections Saddle-Maxima

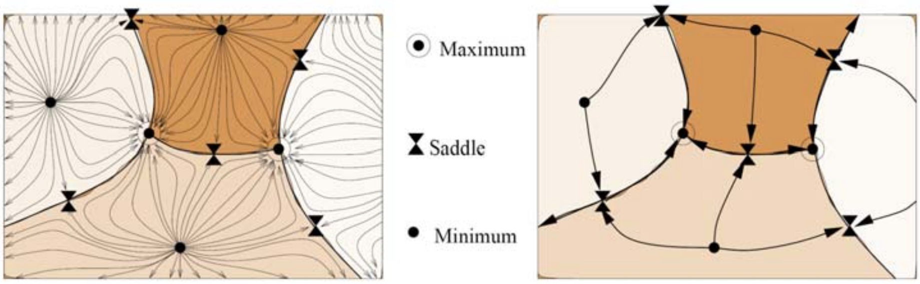

Integral Lines & Field Ridges:

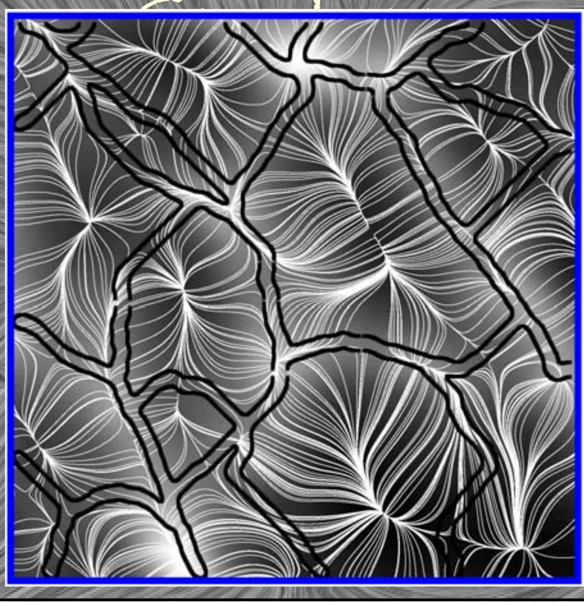

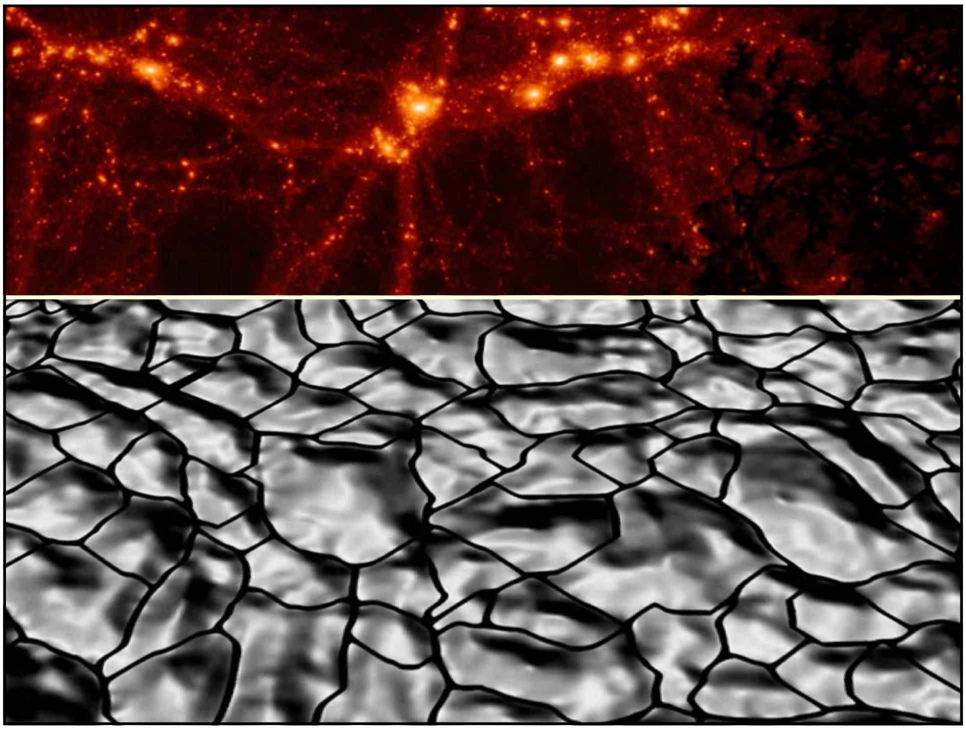

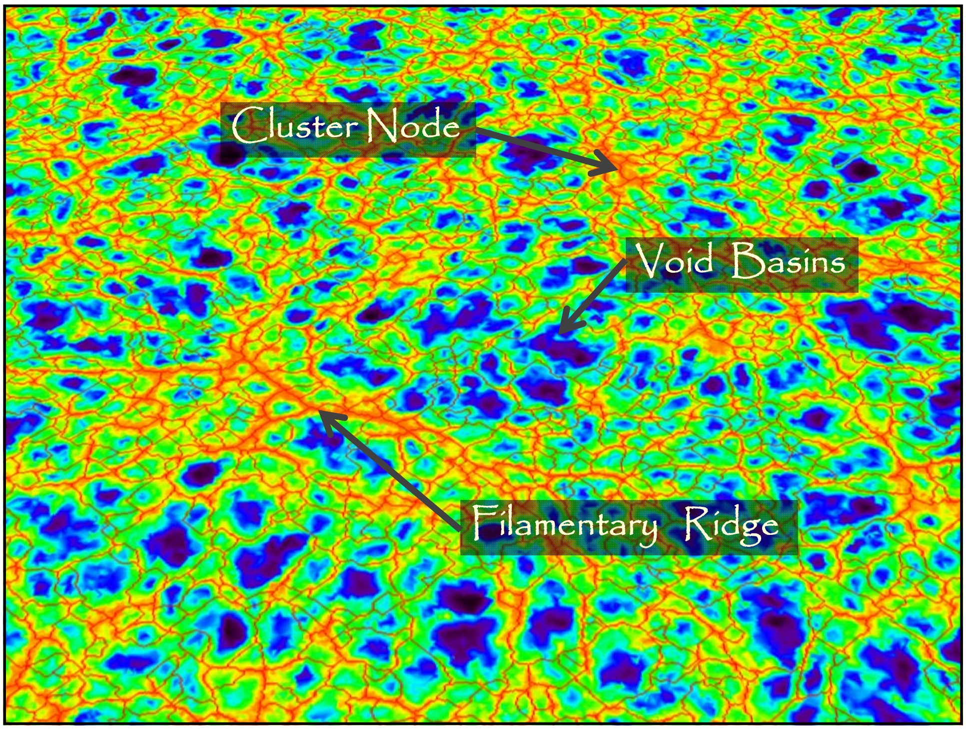
Cluster Node
Void Basins
Filamentary Ridge

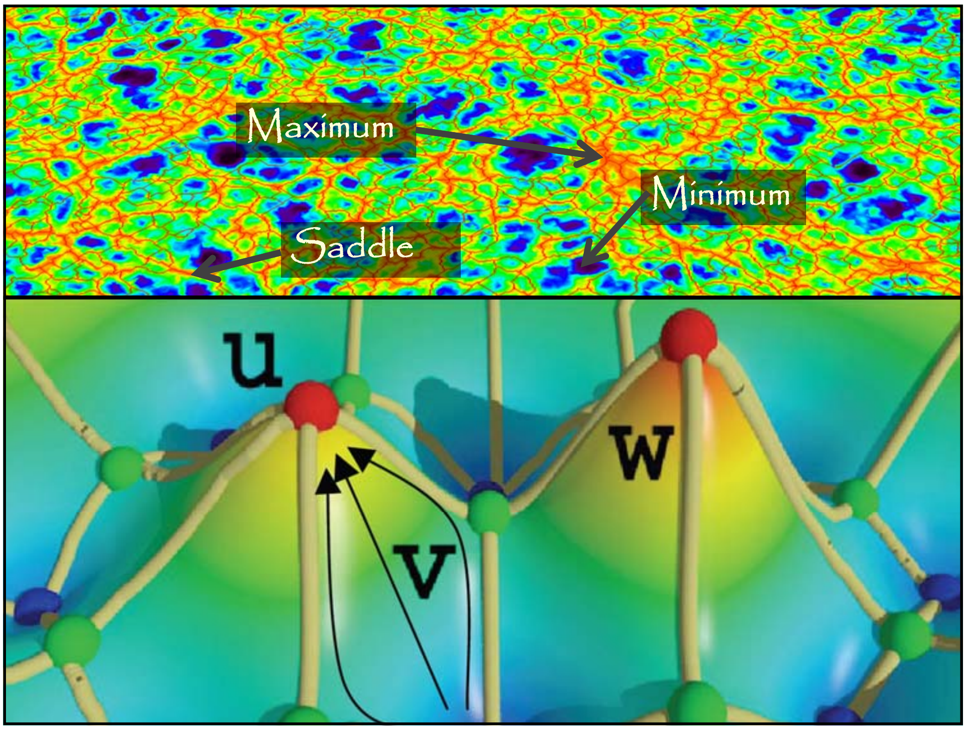
Maximum
Minimum
Saddle
u
w
v